




REPORT

Microscale flow dynamics and particle capture in scleractinian corals: I. Role of the tentacles

Wm. Stephen Price¹ · Mark R. Patterson² 

Received: 5 July 2022 / Accepted: 17 April 2023 / Published online: 3 May 2023
© The Author(s) 2023

Abstract The size, shape, and arrangement of tentacles in scleractinian coral polyps are likely to affect particle capture yet have not been investigated in a systematic way. Morphometric measurements of tentacles of several coral species found in the Caribbean Sea were taken from macro-photographs, and from these, models were constructed in three postures: straight, upstream-facing, and downstream-facing. These models were placed in a flume to video the flow paths of particles around them. Video analysis indicates tentacles, and their specific postures, have a dramatic effect on micro-flow patterns. The expanded soft tissue tentacles, and their specific postures, greatly increase probability of particle capture by direct impaction, inertial impaction, and gravitational deposition. All tentacle postures cause increased retention time relative to freestream travel in their immediate proximity, as well as increasing both contact with the tentacle surface, and tumbling of particles. Straight and upstream-facing tentacles deflect particles downward to their base, while downstream-facing tentacles deflect particles upwards. When results from individual tentacles are considered in geometric combination, the secondary radial symmetry of the tentacular whorls in simple coral polyps appears to be an optimal strategy to filter suspended particulate material in an oscillating and omni-directional flow environment. In meandrine corals, the hedgerows of straight and curved tentacles appear to draw particles downward, retain them, and direct them onto the oral feeding areas below the thecal ridges. The size, shape, and arrangement of tentacles are

thus of key importance in understanding suspension feeding in scleractinian corals.

Résumé La taille, la forme et la disposition des tentacules des polypes des coraux scléactiniaux sont susceptibles d'affecter la capture des particules, mais n'ont pas été étudiées de manière systématique. Des mesures morphométriques des tentacules de plusieurs espèces de coraux trouvées dans la mer des Caraïbes ont été réalisées à partir de macrophotographies et à partir de celles-ci, des modèles ont été construits dans trois postures: droite, orienté à l'amont, et orienté à l'aval. Ces modèles ont été placés dans un canal pour filmer les trajectoires d'écoulement des particules autour d'eux. L'analyse vidéo indique que les tentacules, et leurs postures spécifiques, ont un effet spectaculaire sur les modèles de micro-écoulement. Les tentacules de tissus mous expansés, et leurs postures spécifiques, augmentent considérablement la probabilité de capture des particules par impaction directe, impaction inertielle et dépôt gravitationnel. Toutes les postures des tentacules entraînent une augmentation du temps de rétention par rapport au déplacement du flux libre dans leur proximité immédiate, ainsi qu'une augmentation du contact avec la surface du tentacule et de l'agitation des particules. Les tentacules droits et orientés vers l'amont dévient les particules vers le bas jusqu'à leur base, tandis que les tentacules orientés vers l'aval dévient les particules vers le haut. Lorsque les résultats des tentacules individuels sont considérés en combinaison géométrique, la symétrie secondaire radiale des verticilles tentaculaires des polypes coralliens simples semble être une stratégie optimale pour filtrer les matières particulaires en suspension dans un environnement d'écoulement oscillant et omnidirectionnel. Chez les coraux méandres, les haies de tentacules droits et courbés semblent attirer les particules vers le bas, les retenir et les diriger vers les zones d'alimentation

✉ Mark R. Patterson
m.patterson@northeastern.edu

¹ 1742 Christmas Avenue, Victoria, BC V8P 2X8, Canada

² Marine Science Center, Northeastern University, 430 Nahant Road, Nahant, MA 01908, USA

orales situées sous les crêtes thécales. La taille, la forme et la disposition des tentacules sont donc d'une importance capitale pour comprendre l'alimentation en suspension chez les coraux scléactiniaires.

Keywords Scleractinian coral · Tentacles · Polyp · Suspension feeding · Microscale flow

Introduction

Almost all scleractinian corals are carnivorous, but most species rely primarily on zooxanthellae for energy (Muscatine and Hand 1958; Muscatine and Porter 1977). However, symbiotic algae alone cannot replace nitrogen, phosphorus, and other essential nutrients needed by the coral host; corals must acquire these from other sources, such as zooplankton, particulate organic matter (POM), or dissolved organic matter (DOM) (reviewed by Muscatine and Porter 1977). The prey captured by corals have only been examined in detail for four species of corals, all Caribbean (*Montastraea cavernosa* (Porter 1974); *Meandrina meandrites* (Johnson and Sebens 1993); and *M. cavernosa* and *Madracis mirabilis* and *Porites porites* (Sebens et al. 1998). Even in these studies, questions remain as to the contribution of the marine snow and other hard to measure particulates.

Laboratory and in situ enclosure studies have investigated stomach contents, particle ingestion rates, and flow rates across entire cnidarian colonies (Sebens 1984; Sebens et al. 1997; Sebens and Johnson 1991; Abelson et al. 1993). Although these studies provide critical information on ultimate feeding success, they did not examine the role of polyp morphology in the cnidarian prey capture process. The mechanisms involved in the trapping and transferring of particles to the mouth are still largely a matter of conjecture.

For those corals that appear to filter feed on large, suspended food packets, the filter feeding apparatus consists of circular or longitudinal arrays of delicate, hydrostatically supported tentacles of various sizes and shapes. In many species, these tentacles are photosensitive and remain contracted during the day. This makes direct observations of their role in feeding inherently difficult and may explain why there are so few studies addressing this question (Price 1973; Lewis and Price 1975). Quantitative measurements of parameters affecting encounter and retention of particles have not been recorded for coral tentacles even though examination of the process is deemed critical to a full understanding of the feeding process (Shimeta and Jumars 1991). Thus, information necessary to model capture rates is still lacking for corals.

Because water motion is needed for vigorous coral growth (Darwin 1842; Jokiel 1978; Sebens and Done 1992), it seems most likely that corals have evolved

behavior and morphological features to control flow at the level of the colony, polyp, and tentacle. Rubenstein and Koehl (1977) proposed that most filter feeding mechanisms around individual filter elements are operating in flow regimes of low Re (< 40) where viscous forces become increasingly important and eventually dominate when $Re < 1$. Particles in most suspension feeders are captured using inertial impaction, gravitational deposition, or most commonly, direct interception (Shimeta and Jumars 1991). In calculating Re, most coral studies have described flow in reference to a freestream velocity measured above the colony and used colony diameters or heights as characteristic lengths (Patterson 1984; Helmuth and Sebens 1993). However, these Re values are not applicable to individual coral polyps or tentacles where flow may be dominated by local turbulence and strong velocity gradients. Nowell and Jumars (1984) also suggested that freestream velocity values should not be used to calculate Re for feeding elements, as it is the flow impinging on the filtering element that determines the dynamics of particle interception.

The soft tissue structure of the polyps reflects the complexity of the corallites. The tentacles, which can be considered as the fundamental feeding elements, are also found in a wide variety of sizes, shapes, and complex configurations. How these patterns are related to feeding and other behavioral functions is not understood, nor have their influence on microscale flow dynamics received attention except for some preliminary work by Price (1973). This study examines the role of tentacle length and posture in the feeding of corals and in particular addresses the following questions:

- (1) Are the tentacle lengths correlated with the flow habitat where each species is most commonly found?
- (2) What are the approximate Re for flow around tentacles, and is there a predictable range of Re across which they appear to function?
- (3) Are deflection, retention, and contact dependent on tentacle posture?
- (4) Could elongated "sweeper tentacles" enhance filter feeding?
- (5) What are the synergistic consequences of different tentacle arrangements found in polyps?

Dynamic similarity states that the flow patterns around physically similar objects will be the same if the Re of the two systems, the organism in nature and the physical model in the laboratory, is the same (Vogel 1983). Physical modeling of tentacles not only allows working at larger scales for easier observation, but also for isolation and manipulation of their transient positions. We now describe how physical models were implemented to answer the questions posed above.

Materials and methods

Models of coral tentacles

Morphometric measurements of tentacles were collected from underwater macro-photographs (magnification 1:1, 1:2, and 1:3) of 27 Caribbean coral species found in Barbados, and St. Vincent and the Grenadines (Table 1). The base, middle, and distal tentacle diameters, as well as tentacle lengths, were measured from photographic transparencies using a dissecting microscope. Tentacles, being hydrostatically supported soft tissue structures, are inherently variable in form. Tentacle lengths and diameters are affected by different flow regimes, irradiance levels, and diver disturbance (personal observations). Consequently, measurements of at least 10 tentacles in five different polyps were averaged from within several polyps of a single colony and between two different colonies.

The *characteristic length* used to calculate the Reynolds number (Re) was taken as the greatest length of an object in the direction of the flow. Because tentacle positions vary across a polyp and colony, the tentacle length was used as this characteristic length for Re calculations. The length of the tentacle is an appropriate characteristic length as the moving water in proximity to the tentacle feels the viscous forces exerted on it, and vice versa. As noted below, we gathered flow speeds from the region next to the tentacles for the computation of Re , as our concern is how flow around tentacles impacts particle capture.

For this study, Re was computed for objects in moving water, following Vogel (1983):

$$Re(\text{dimensionless}) = \frac{(1/\eta) (\text{s cm}^{-2}) \times \text{characteristic length (cm)} \times \text{flow speed (cm s}^{-1})}{1} \quad (1)$$

For water, $\eta = 0.01 \text{ cm}^2 \text{ s}^{-1}$, approximately.

The range of tentacle types of both simple and meandrine polyps was typified by two postures: *straight* and *curved*. Since the flow over a reef is oscillatory and omni-directional, tentacles curved upstream into the flow during the first half of the oscillation are curved *downstream* with the flow in the next half oscillation. Thus, three postures were defined: *straight*, *upstream-facing*, and *downstream-facing* (Fig. 1). These generic postures were modeled in *Super Sculpey*™ approximately 10x life size (7 cm in length). Elongated *sweeper* tentacles, which are occasionally found on the periphery of *Agaricia agaricites* and *Montastraea cavernosa* colonies (Price 1973), were also modeled approximately 10x life size (Fig. 2).

Flow speeds

Microscale flow speeds were video-recorded over the surface of expanded colonies of *Montastraea cavernosa*, *Colpophyllia natans*, *Siderastraea siderea*, *Meandrina meandrites*, *Diploria labyrinthiformis*, and *Dichocoenia stokesii*, at 20 m depth at Conch Reef (24.57°N, 80.28°W) off Key Largo, Florida, USA. A Sony V-99 Hi-8 mm video camera in an underwater housing was weighted and held on the substrate at right angles to the oscillating flow, and then manually focused on polyps 10 cm from the macro lens port. An opaque PVC disk with a 2-mm-wide slit opening, fitted on a standard dive light, produced a collimated light sheet that illuminated a 1-cm depth of field (Fig. 3). The trajectories of five particles above each of the 12 different coral heads were measured using frame-by-frame video analysis.

Flume

A transportable laminar flow 100-liter flume, two meters in length, was constructed for the project (Fig. 4). The working trough was made of four 50-cm-long clear acrylic sections (15 cm × 15 cm), bolted together in tandem. Flow speeds were controlled by a Bodine Series 400, 1/15 hp motor driving a 12-cm-diameter, double-bladed, plastic propeller. To straighten the flow, longitudinal plates were built within the return pipes to eliminate most of the secondary flow from the propeller. When the flow entered the flume, it passed through four honeycomb Aeroflex™ blocks (5 cm thick with 5 mm channels).

The tentacle models were placed in the third section of the flume where flow was the most uniform. The wall boundary layer effects could be considered negligible since the projected surface area of the models normal to the flow was less than 2 percent of the cross-sectional area of the flume (Nowell and Jumars 1984; Denny 1988). To reduce the influence of the floor boundary layer, the tentacle was affixed 2 cm above a grid-marked PVC “substrate” platform, on a narrow (2-mm-dia.) stainless steel bolt.

Tracer particles and video analysis

To investigate the motion of particles around the models, finely chopped bean sprout disks (c. 1 mm thick), stained opaque with Tintex™ black fabric dye, were used. They had a mean ($n = 50$) sinking velocity of 0.25 cm s^{-1} , similar to mucus flocks (0.2 cm s^{-1} ; Johannes 1967). The relative density (difference between the fresh-water used in the flume and the particle) was of order

Table 1 Tentacle lengths, Reynolds numbers (Res), depth distribution, and diurnal polyp expansion, of 27 Caribbean corals

Species used for study	Tentacle Length (cm)	Expanded Day/Night	Optimal depth**			Depth General	Habitat Flow	Re @			
			Min	Max	Optimum			5 cm s ⁻¹	10 cm s ⁻¹	25 cm s ⁻¹	50 cm s ⁻¹
<i>Agaricia lamarcki</i>	0.05	Day & Night	22 ²	56 ²	22–56 ²	Deep	Slow	25	50	125	250
<i>Agaricia agaricites</i>	0.06	Day & Night	1 ¹	45 ¹	7–20 ¹	Shallow	Fast/Moderate	30	60	150	300
<i>Acropora palmata</i>	0.09	Day & Night	1 ¹	17 ¹	1–5 ¹	Shallow	Fast	45	90	225	450
<i>Montastraea annularis</i>	0.10	Day & Night	0.3 ¹	80 ¹	3–45 ¹	Shallow	Fast	50	100	250	500
<i>Acropora cervicornis</i>	0.11	Day & Night	0 ¹	50 ¹	15–30 ¹	Mid	Moderate	55	110	275	550
<i>Diploria clivosa</i>	0.11	Day & Night	0 ¹	10 ¹	1–3 ¹	Shallow	Fast	55	110	275	550
<i>Porites porites</i>	0.12	Day & Night	0.5 ¹	20 ²	5–10 ³	Shallow	Fast	60	120	300	600
<i>Siderastrea sideraea*</i>	0.12	Day & Night	0.5 ¹	70 ¹	3–20 ¹	Shallow	Fast	60	120	300	600
<i>Porites astreoides</i>	0.13	Day & Night	0.2 ¹	70 ¹	5–20 ¹	Shallow	Fast	65	130	325	650
<i>Stephanocoenia michelini</i>	0.14	Day & Night	1 ¹	95 ¹	3–50 ¹	Shallow/Mid	Fast/Moderate	70	140	350	700
<i>Mycetophyllia lamarckiana</i>	0.17	Night	1 ¹	70 ¹	5–40 ¹	Mid/Deep	Slow	85	170	425	850
<i>Mycetophyllia aliciae</i>	0.19	Night	20 ³	56 ²	25–40 ³	Mid/Deep	Slow	95	190	475	950
<i>Favia fragum</i>	0.23	Day & Night	0.2 ¹	30 ¹	2–8 ¹	Shallow	Fast	115	230	575	1150
<i>Mycetophyllia danaana</i>	0.30	Night	25 ³	40 ³	25–40 ³	Deep	Slow	150	300	750	1500
<i>Oculina diffusa</i>	0.32	Day & Night	20 ³	40 ³	20–40 ³	Deep	Slow	160	320	800	1600
<i>Montastraea cavernosa* (side)</i>	0.38	Night	0.5 ¹	95 ¹	10–60 ¹	Mid/Deep	Moderate	180	360	900	1800
<i>Diploria labyrinthiformis</i>	0.40	Night	0 ¹	43 ¹	2–15 ¹	Mid	Moderate	375	750	1875	3750
<i>Diploria strigosa*</i>	0.43	Night	0 ¹	40 ¹	3–10 ¹	Mid	Moderate	215	430	1075	2150
<i>Scolymia cubensis</i>	0.54	Night	15 ¹	30 ¹	30–50 ¹	Deep	Slow	270	540	1350	2700
<i>Meandrina meandrites*</i>	0.60	Night	0.5 ¹	70 ¹	8–30 ¹	Mid	Moderate	505	1010	2525	5050
<i>Montastraea cavernosa* (top)</i>	0.65	Night	0.5 ¹	95 ¹	10–60 ¹	Mid/Deep	Moderate	625	1250	3125	6250
<i>Colpophyllia natans*</i>	0.70	Night	0.5 ¹	55 ¹	2–20 ¹	Mid	Moderate	300	600	1500	3000
<i>Isophyllastrea multiflora</i>	0.70	Night	20 ³	40 ³	20–40 ³	Deep	Slow	300	600	1500	3000
<i>Eusmilia fastigiata</i>	0.71	Night	1 ¹	65 ¹	3–30 ¹	Shallow/Mid	Slow/Moderate	355	710	1775	3550
<i>Agaricia agaricites (sweeper)</i>	0.80	Night	1 ¹	45 ¹	7–20 ¹	Shallow	Fast/Moderate	400	800	2000	4000
<i>Dichocoenia stokesii*</i>	0.85	Night	2 ¹	40 ¹	3–2 ¹	Mid/Deep	Moderate	425	850	2125	4250
<i>Dendrogya cylindrus</i>	1.15	Day & Night	2 ¹	20 ¹	3–8 ¹	Mid	Moderate	575	1150	2875	5750
<i>Mussa angulosa</i>	1.2	Night	1.5 ¹	59 ¹	10–30 ¹	Deep	Slow	600	1200	3000	6000
<i>Tubastraea coccinea (top)</i>	1.3	Day & Night	0.3 ¹	35 ¹	1.5–25 ¹	Mid	Slow	300	600	1500	3000
<i>Montastraea cavernosa (sweeper)</i>	5.0	Night	0.5 ¹	95 ¹	10–60 ¹	Mid	Moderate	2500	5000	12,500	50,000
<i>Normal tentacle models</i>	7.0					Flume		3500			
<i>Sweeper tentacle model</i>	35					Flume		2500			

Tentacle length is the mean length of 10 tentacles of 5 different polyps

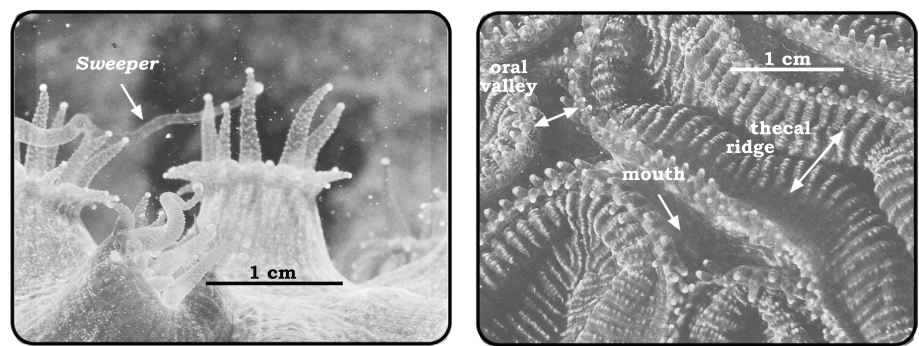
Side: tentacle whorl at right angle to polyp column *Top*: tentacle whorl at right angle to polyp oral disk

Flow speeds cover the range reported by Sebens et al. (1997)

*Species video-recorded at 20 m depth (Florida) and analyzed for flow speed

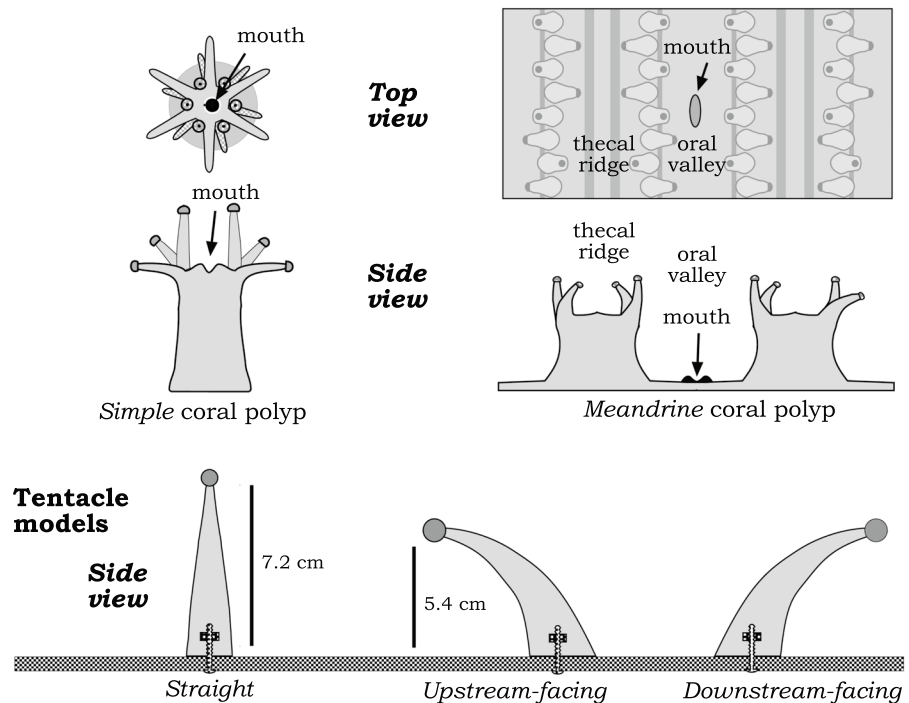
**Depth values are taken from: ¹Goreau and Wells (1967); ²Liddell and Ohlhorst (1987); ³the authors

Fig. 1 Macro-photographs of *Montastraea cavernosa* (a) and *Colpophyllia natans* (b) followed by simplified top and side views of polyp models, and side views of the tentacle models with dimensions



(a) *Montastraea cavernosa*

(b) *Colpophyllia natans*



$10^{-2} \text{ g cm}^{-3}$, which places them close to invertebrate larvae ($3.2 \times 10^{-2} \text{ g cm}^{-3}$; Salzen 1957) (Table 2). Scaled to the models, they are equivalent to particles 100–200 μm , or the size of many invertebrate larvae (Butman 1986).

Video recordings were made using a Sony video camera. A mirror above the flume allowed for simultaneous recording in both the vertical (xz -axis) and horizontal (xy -axis) planes. Frame-by-frame (1/30th s) analyses (position resolution 1 mm) of the paths of 10 particles encountering each vertical z one of the three tentacle postures were performed in both the horizontal and vertical planes from pre-encounter to several tentacle diameters post-encounter (Fig. 2).

Defining horizontal regions and vertical zones of influence

Horizontal travel

Two scales of horizontal (xz -axis) particle travel were used. A coarse scale divided the horizontal recordings into four, 5-cm, equidistant horizontal *regions* (I–IV) from pre-encounter to post-encounter. Because the behavior of particles close to the tentacle is important in determining the probability of capture by the tentacle, a second scale consisting of an *inner region*, extending one local radius downstream, and an *outer region*, extending to three radii beyond this (Fig. 2) was defined.

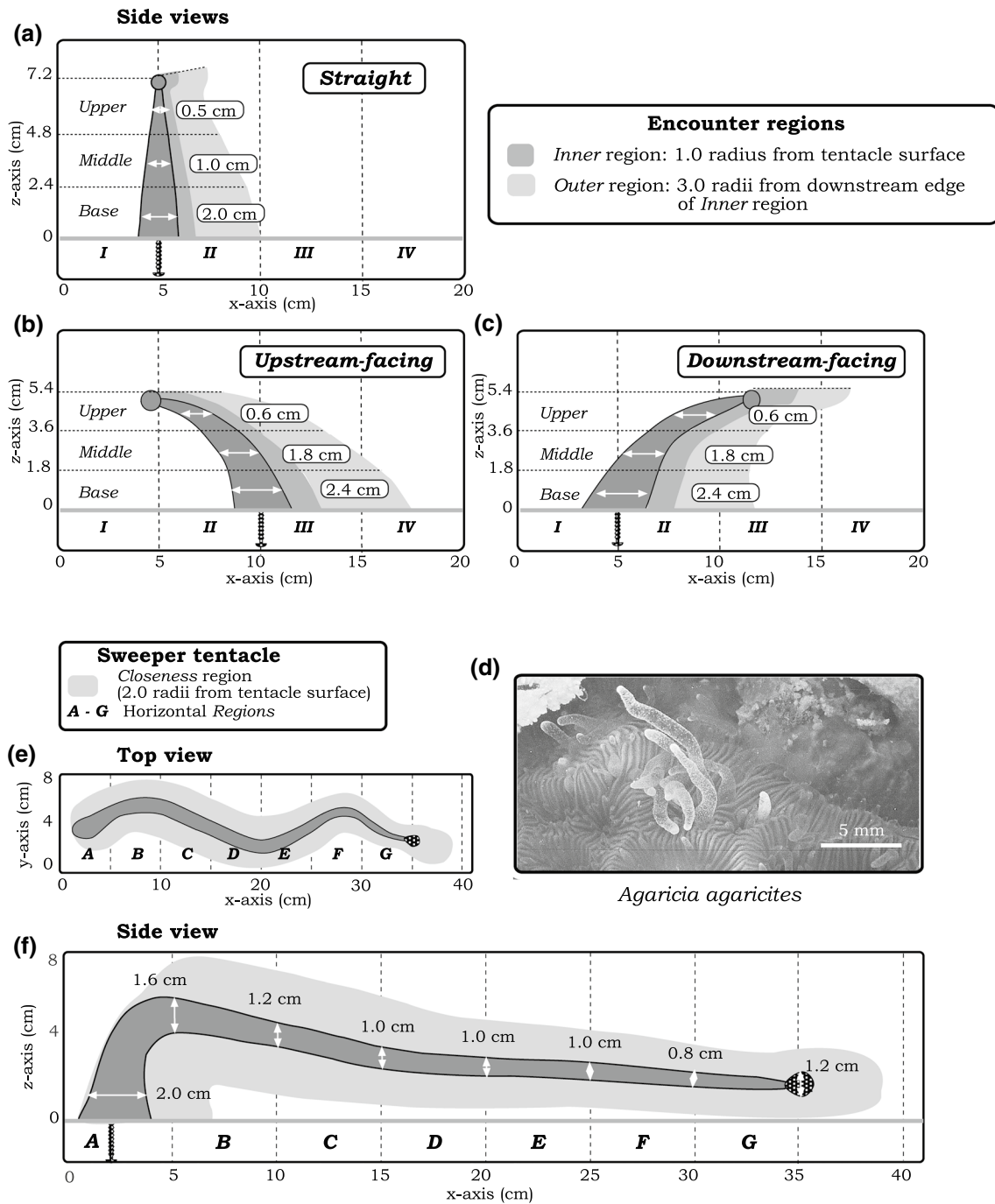


Fig. 2 Vertical encounter zones around model tentacles (upper, middle, base) and the inner (○) (1.0 local tentacle radius) and outer horizontal region (○) (3.0 local tentacle radii from top of inner horizontal region) for the three postures of coral tentacles: straight (a), upstream-facing (b), and downstream-facing (c). Local tentacle diameters (white double-arrows) indicated on diagram inside the

ellipses. Note that the total extent of the inner and outer horizontal regions totals to 4 tentacle radii and is height dependent. Also, the upstream horizontal region where encounter speeds were measured extends 10 cm for all models, thus farther than the 5 cm implied by the location of the model diagrams. For sweeper tentacles (d), closeness and horizontal regions are presented in top (e) and side (f) view

Fig. 3 Recordings were made of corals at night to measure micro-flow regimes around and above expanded tentacles. A collimated light sheet, oriented parallel to the flow, illuminated particles in the water and around a band of polyps. The width of the light sheet (perpendicular to the flow direction) just above the polyps was about 1 cm

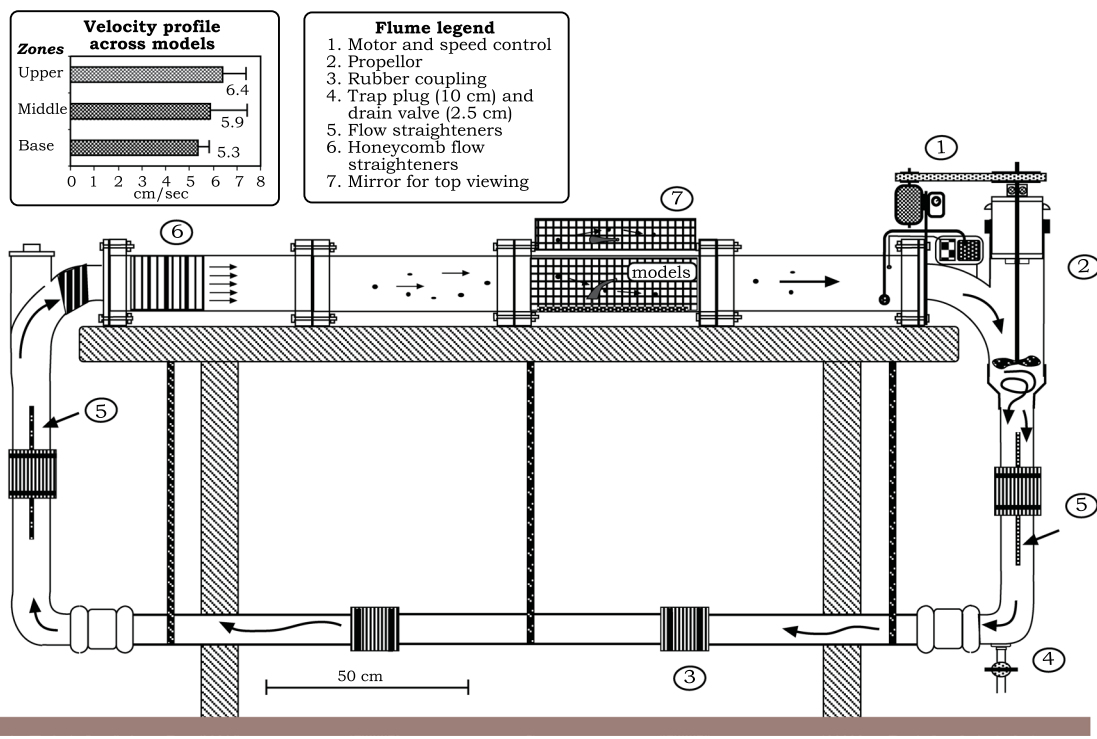
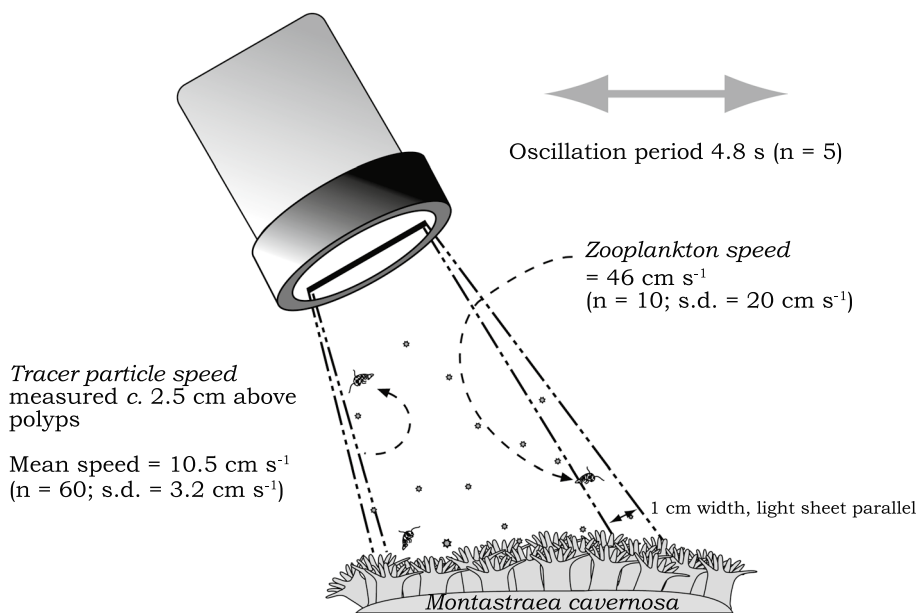


Fig. 4 Portable laminar flume used to observe flow patterns around models of coral tentacles. Left inset: average speed profiles+SD ($n=30$) as function of height in the upper, middle, and base vertical

zones, as defined in Fig. 2. Right inset: key for the components of the recirculating flume

Vertical travel

The vertical aspect of the tentacle was divided into three equal vertical zones, termed *upper*, *middle*, and *base*. For the straight tentacle, this made the *upper zone* from 4.8 to

7.2 cm; the *middle zone* from 2.4 to 4.8 cm; and the *base zone* from 0.0 to 2.4 cm. In the two curved models, the dimensions for the *upper*, *middle*, and *base vertical zones* were 3.6–5.4 cm, 1.8–3.6 cm, and 0.0–1.8 cm, respectively (Fig. 3).

Table 2 Size, density, and sinking velocity for various marine suspended particulates and tracer particles (sprout slices, $n=50$) used for the study

Particle type	Size of particle r_p (μm)	Density differential $\rho_p - \rho$ (g cm^{-3})	Sinking velocity w_s (cm s^{-1})	Reference
Fine sand	75	1.63	2.0	Shimeta and Jumars (1991)
Organic-mineral aggregate	50	8.8×10^{-2}	5.0×10^{-2}	Gibbs (1985)
Small phytoplankton	5.0	6.9×10^{-2}	3.4×10^{-6}	Jackson (1989)
Experimental tracer particles	100–200	$O(1.0 \times 10^{-3})$	0.25	This study
Invertebrate larvae	250	7.3×10^{-3}	0.1	Butman (1986)
Large phytoplankton	50	9.0×10^{-3}	5.0×10^{-3}	Jackson (1989)
Marine snow	2500	6.5×10^{-5}	8.8×10^{-2}	Allredge and Gotschalk (1988)

Computation of particle travel parameters

Particle trajectory distribution

Particles encountering the tentacles within any of the three vertical zones hypothetically could go through any of the *inner* and *outer horizontal regions*. Particles that passed through these horizontal regions were expressed as a percentage of the potential 10 particles that hypothetically could enter each vertical zone.

Vertical deflection

The vertical deflection was measured as the difference between *inner horizontal region* entry point and the region (*inner* or *outer*) exit point on the z -axis, with upward deflections positive and downward deflections negative. Particle travel paths were not recorded below the tentacle base.

Horizontal deflection: encounter width and particle spread

The cross-stream width of an ensemble of particles before they encountered the tentacles models was measured from path tracings performed 5 cm in front of the tentacle. We call this cross-stream width and the *encounter* width, and we categorized these widths by the particle approach position on the xy -plane in three horizontal radial regions: (i) within 1.0 local tentacle diameter; (ii) between 1.0 and 1.5 local tentacle diameters; and (iii) beyond 1.5 local tentacle diameters.

Similarly, the cross-stream width post-encounter with the tentacle was measured from an ensemble of particles at approximately five local diameters d_p , downstream of the models. The width was taken as the distance from the central axis of the tentacle to the position of the furthest trace path on either side. This distance was then doubled and then transformed into a dimensionless post-encounter spread ratio (d_s):

$$d_s(\text{dimensionless}) = \frac{\text{post-encounter spread (cm)}}{\text{pre-encounter diameter (cm)}} \quad (2)$$

For example, if the furthest post-encounter spread measured was 3.6 cm at the base vertical zone of the tentacle, where the local diameter is 2.4 cm, the dimensionless spread value d_s is $2(3.6 \text{ cm})/2.4 \text{ cm}$, or 3.0.

Time and retention value (r)

The *actual time* t_a , a particle spent within a given *region*, was measured with a resolution of 1/30 s. The speed at which the particle approached the tentacle (measured 10 cm upstream of the tentacle over 10 frames of video), we call the *encounter speed* v_e . We endeavored to set this speed to approximately 5 cm s^{-1} in the middle of the base zone, but it ranged $4.5\text{--}7.5 \text{ cm s}^{-1}$ because of differences of particle release height in the boundary layer and variations in the flume speed controller (inset, Fig. 4). To allow use of particles approaching at speeds other than 5 cm s^{-1} , we compensated for this experimental variability by normalizing the tracking times of the particles as follows. The time a particle spent in each region was multiplied by the ratio of the actual encounter speed to a *standardized speed* v_s of 5.0 cm s^{-1} . We thus defined a transformed time (t_t):

$$t_t(\text{s}) = t_a(v_e/v_s) \quad (3)$$

Thus, if a particle encountered the tentacle at 7 cm s^{-1} , then the actual time that this particle spent in each region would be multiplied by a factor of $(7/5)$ to yield the transformed time.

To calculate retention effects, in the absence of the physical model, it was assumed that particles would have continued in straight-line paths at the (adjusted) freestream velocity. Thus, any distance a particle traveled along the horizontal axis would have a theoretical *freestream time* t_s -value.

We then defined a dimensionless *retention value* (r):

$$r(\text{dimensionless}) = t_r(s)/t_s(s) \quad (4)$$

If an r -value is < 1 , the particle must have been accelerated as it traveled around the tentacle. Note, if the r -value > 1 , this cannot be equated to a reduction in speed as actual travel distance in a vortex could be much longer than a straight-line freestream distance. However, higher values of r indicate an increase of time spent in the vicinity of the tentacle which would increase the probability of particle capture. In the event of a particle stalling, or prolonged contact against the tentacle surface, the stall time was subtracted from the calculation. This makes the calculation of the r -value conservative. Also, when a particle dropped below the tentacle base (“0” on the z -axis), tracking was terminated.

Particle contacts and rotations

Contacts of particles with the surface of the tentacle were recorded as either a direct frontal *impact contact*, or if the contact occurred on the downstream side of the tentacle, as a *vortex contact*. A *rotation* was defined as an event in which a particle looped or rotated around its axis as it moved horizontally.

Sweeper tentacle

Particles ($n = 24$) traveling along the elongated *sweeper* tentacle were tracked on the horizontal axis of the tentacle model through seven 5-cm horizontal regions (A–G) (Fig. 2). However, since the diameter of the *sweeper* tentacle decreased from the base to its tip, the proximity of the particle from the tentacle surface was divided by the local diameter of the tentacle (Fig. 2) to define a dimensionless closeness value (d_{cl}):

$$d_{cl}(\text{dimensionless}) = \text{proximity (cm)}/\text{local diameter (cm)} \quad (5)$$

The straight-line three-dimensional diagonal distance between exit and entry points of the 5-cm horizontal regions was calculated and then summed to give a conservative estimate of the total travel distance of a particle. The particle retention r -value was calculated as the time spent in each region, transformed to the standardized encounter velocity of 5 cm s^{-1} , and then expressed as a ratio of the freestream time for a particle to cover the same distance. Also, a particle path that crossed over the axis of the tentacle was recorded as a distinct “crossing” event.

Results

Tentacle posture, flow rates, and Re for tentacles

The length of normal tentacles ranged from 0.05 to 1.3 cm (Table 1) in the coral species examined. Sweeper tentacles, 4 and 20 times the length of normal tentacles were measured in *Montastraea cavernosa* (4–6 cm) and *Agaricia agaricites* (0.6–1.1 cm), respectively. Examination of the macro-photographs of both simple and meandroid corals indicated that polyps could be considered as having combinations of *curved* and *straight* tentacle whorls or rows. In the simple polyps, such as *Montastraea cavernosa* or *Tubastraea coccinea*, in addition to the *curved* tentacles, there are whorls of *straight* tentacles perpendicular to the plane of the oral disk, as well as horizontal-*straight* tentacles parallel to the plane of the oral disk (Fig. 1). In both these species, the vertical-*straight* tentacles were found to be double the length of the horizontal-*straight* tentacles (Table 1). In contrast, for the meandroid coral, such as in *Diploria labyrinthiformis*, the vertical-*straight* tentacles found on the thecal ridge were approximately 30% shorter than the more horizontal-*curved* tentacles (7.5 mm compared to 10.5 mm).

No correlation was found between the optimum depth at which a coral species was found and tentacle length ($R^2 = -0.08$). Flow environments could only be divided qualitatively into three broad categories: *fast-flow* as found in exposed inshore shallow area (1–5 m depth); *moderate-flow* for the mid-reef area (5–20 m depth); and *slow-flow* deep-reef (20–35 m depth). In general, however, coral species found in the shallow and *fast-flow* habitat have short tentacles ($< 0.15 \text{ cm}$) which remain expanded during the day and night. The *moderate-flow* mid-reef areas are dominated by longer tentacled species that fully expand their polyps at night. In the *slow-flow* deep habitats, short tentacled species seem to be dominant and they too generally expand their tentacles only at night. However, in this deeper zone, very long tentacled species, such as *Mussa angulosa* and *Scolymia cubensis* are also found, and they too fully expand only at night (Table 1).

Flow speeds over the colonies of *Montastraea cavernosa*, *Colpophyllia natans*, *Siderastrea siderea*, *Meandrina meandrites*, *Diploria labyrinthiformis*, and *Dichocoenia stockesii*, filmed at a depth of 20 m averaged $10.7 \pm 3.2 \text{ cm s}^{-1}$ (mean \pm SD; $n = 60$), with an oscillatory period of 4.8 s ($n = 5$). Flow speeds within the tentacles and up to 5 cm above the expanded polyps showed no gradient. Numerous unidentified large zooplankton were attracted to the video light swimming at an average speed of $46 \pm 20 \text{ cm s}^{-1}$ (mean \pm SD; $n = 10$). Using the similar flow

rate of 10 cm s^{-1} , the Re of the six species ranged from 120 to 1250 (Table 1). Since accurate flow rates are not available for all species, and to cover the range of flow speeds that they would normally experience, Re values were calculated at 5, 10, 25, and 50 cm s^{-1} (Table 1). All the calculated Res are \gg and most are well above $Re = 40$, ranging up to 6250 (*M. cavernosa*, “top” tentacles).

Tentacle models

The average flow speed in the flume was set to be approximately 5.0 cm s^{-1} , which gave a Re for the models as 3500. This is in the range of the Re encountered by medium to long tentacles in moderate- to high-flow environments and therefore produced similar flow characteristics. The boundary

layer descriptions and turbulence intensities for this flume are given in dimensionless form in Patterson (1984).

Particle distribution through horizontal regions as percent occurrence

All particle traces ($n=90$) are presented in a composite of posture and encounter vertical zones in Fig. 5, and percentage computations of particle trajectories are shown in Fig. 6. For the *straight* tentacle, all particles encountering the *upper zone* tended to stay within the *upper* encounter zones immediately after passing by the tentacles. Only one dropped into the *outer middle zone* within the *outer region*. *Middle-zone* encounters caused 10% of the particles to drop into the *inner base* horizontal region and 40% to pass through the *outer base* horizontal region. All particles encountering the *base*

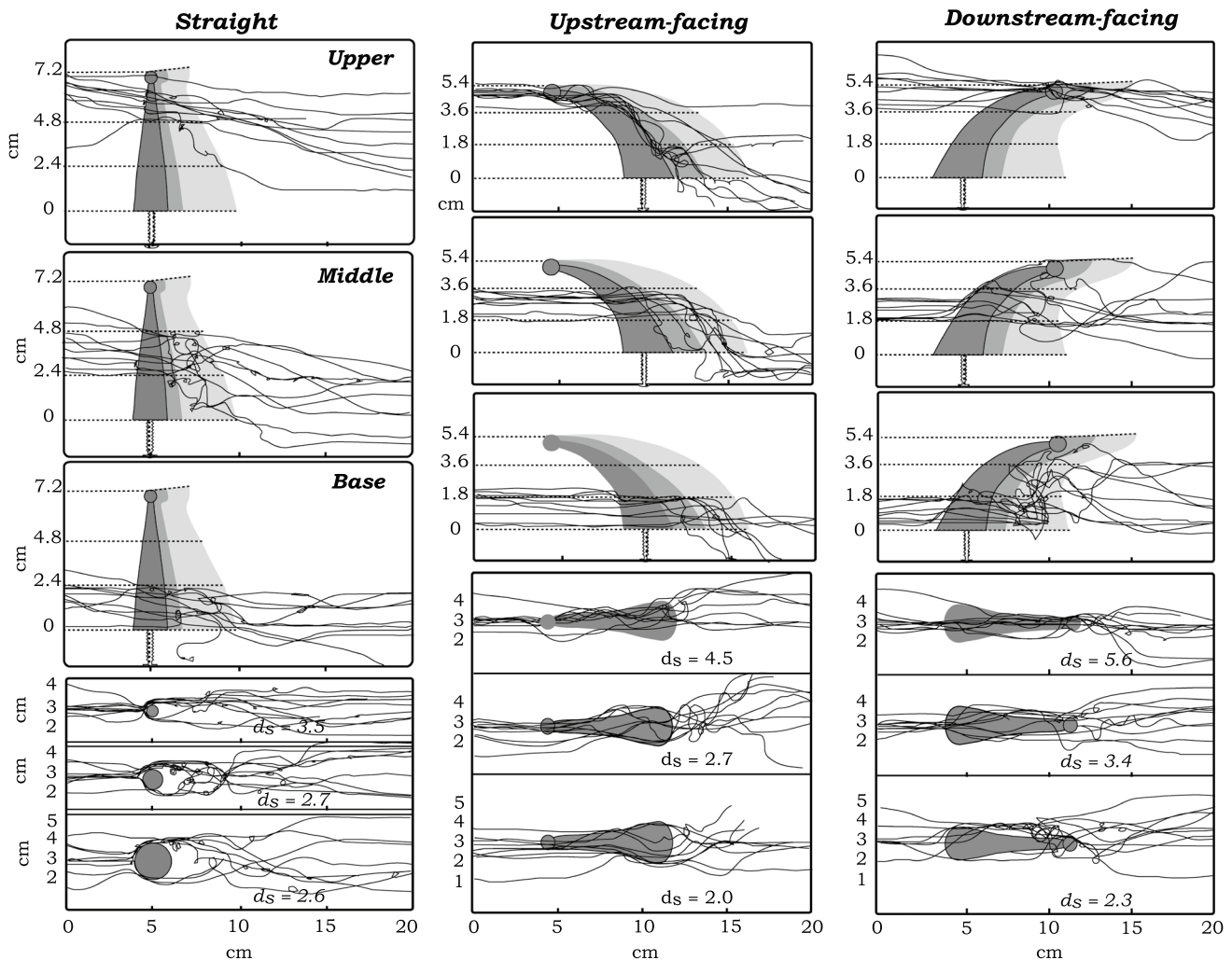


Fig. 5 The particle traces through the inner (<1.0 local tentacle diameter) (\square) and outer (>3.0 local tentacle radii from top of inner) (\square) horizontal regions of the three tentacle posture models, in the upper, middle, and base approach sections. Travel along the vertical

($x-z$ axes) and horizontal ($x-y$ axes) planes is shown for the same particle sets ($n=10$ for each vertical zone and each posture). The dimensionless spread ratio values (d_s) are expressed as mean for $N=10$ particles traced

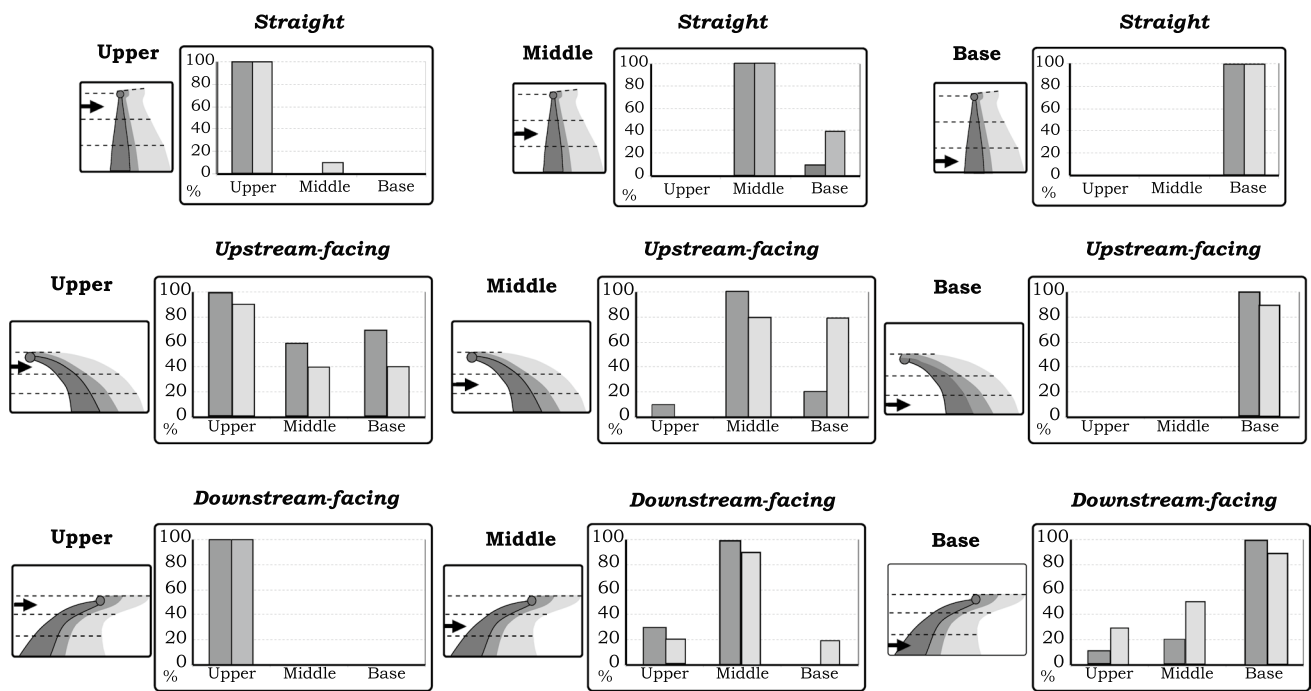


Fig. 6 The distribution of particles (% occurrence) through the inner and outer horizontal regions as defined in Fig. 5 after encountering the different tentacle postures within the three vertical zones (upper,

middle, base). Arrows denote direction of flow at midpoint of the vertical encounter zones. In each vertical zone, 10 particles were traced for each tentacle posture

vertical zone passed through both *inner* and *outer horizontal regions* (Fig. 6).

Particles that encountered the *upper vertical zone* of the *upstream-facing* tentacle resulted in particles passing through all six post-encounter horizontal regions. *Middle-zone* encounters also spread particle distribution, but mostly in the *outer middle* and *base* horizontal regions. Base encounters resulted in particles remaining in the *base vertical zone*.

Particles encountering the *downstream-facing* tentacle influenced flow reacted quite differently. *Upper-zone* encounters caused 100% of the particles be retained in both *upper horizontal regions*. However, *middle-zone* encounters caused 30% of the particles to be deflected upwards into the *upper inner horizontal region* and 20% into the *upper outer horizontal region*. Very few dropped into the base horizontal regions. *Base-zone* encounters caused particles to be deflected into all six *horizontal regions*.

Deflection: horizontal and vertical

Vertical deflection

Vertical deflection values across the *inner* and *outer horizontal regions* are presented in Fig. 7. The *straight* tentacle produced a downward deflection in all three vertical encounter zones with the *middle zone* having a slightly greater effect. The *upstream-facing* tentacle produced strong downward

displacement of particles along its entire length, with the *upper horizontal regions* causing a strong deflection of an average of 3.8 cm, of the 5.4 cm high model. For the *downstream-facing* model, there was effectively no downward vertical displacement in either the *upper* or *middle vertical zones*. However, there was strong upward lift from the *base-zone* encounters of 1.2 cm.

Horizontal deflection

Most of the particles (79%) that were influenced by the tentacle models approached within one tentacle diameter irrespective of the approach height (Fig. 8). Of the remainder, 12% were within 1.5 diameters and 9% beyond this width.

The average post-encounter spread values across the three vertical zones were similar for all three tentacle postures (*straight*, $d_s = 2.9$; *upstream-facing*, $d_s = 3.0$; and *downstream-facing*, $d_s = 3.8$). However, the spread for each vertical zone showed a different pattern from one posture to another (Fig. 8).

Particle retention (r)

Coarse-scale retention: horizontal regions

Retention was only slightly positive in the first encounter horizontal regions of all three postures ($r = 1.1$) but

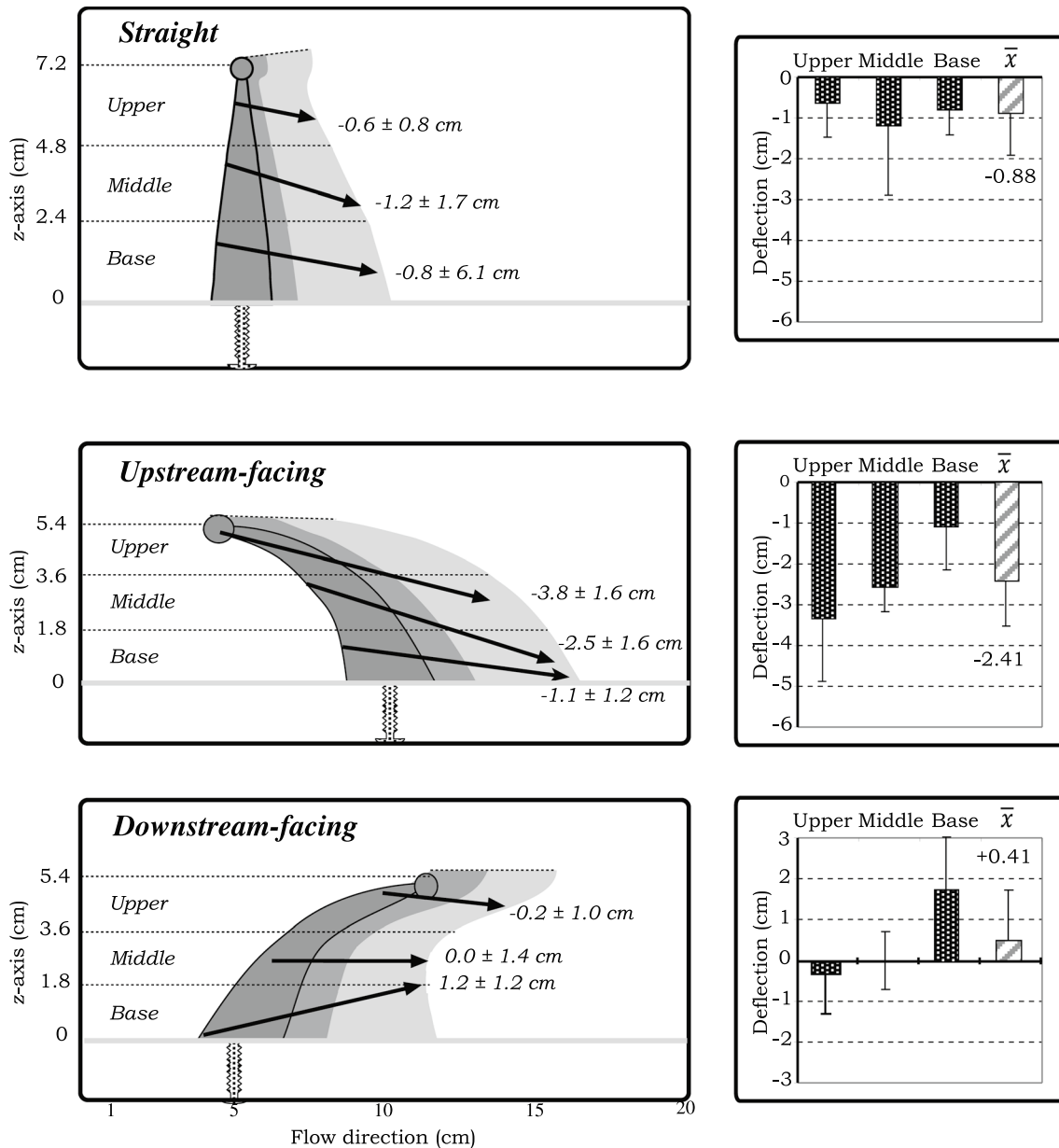


Fig. 7 Vertical deflection of particles across the inner and outer horizontal regions following encounter with the different tentacle postures. Downward deflection is (–) and upward deflection is (+). Mean \pm standard deviation (cm) of particles

was immediately increased in the subsequent two post-encounter regions (Fig. 9). The *upstream-facing* tentacle produced the strongest effect in both post-encounter horizontal regions II and III ($r=1.8$ and 2.5 , respectively). In the *straight* tentacle regions, $r=1.7$ (II) and $r=1.6$ (III), and the *downstream-facing* tentacle retention was slightly less, where both r -values equaled 1.5 . By horizontal region IV (beyond 10 cm), most particles, except for those that had dropped below the baseline, were returning to freestream velocities.

Fine-scale retention—inner and outer horizontal regions

Straight tentacle: *Upper-zone* encounters had moderate average retention of *inner* r -value = 1.7 and *outer* r -value = 1.4 , except for one particle that accelerated through the *outer middle horizontal region* for an r -value = 0.5 (Fig. 10). *Middle-zone* encounters had a relatively low *inner* retention r -value ($r=1.2$) but had a much higher *outer* value ($r=2.9$). One particle was retained in the *inner base region* for a long period for an r -value of 14.0 . Particles encountering the *base*

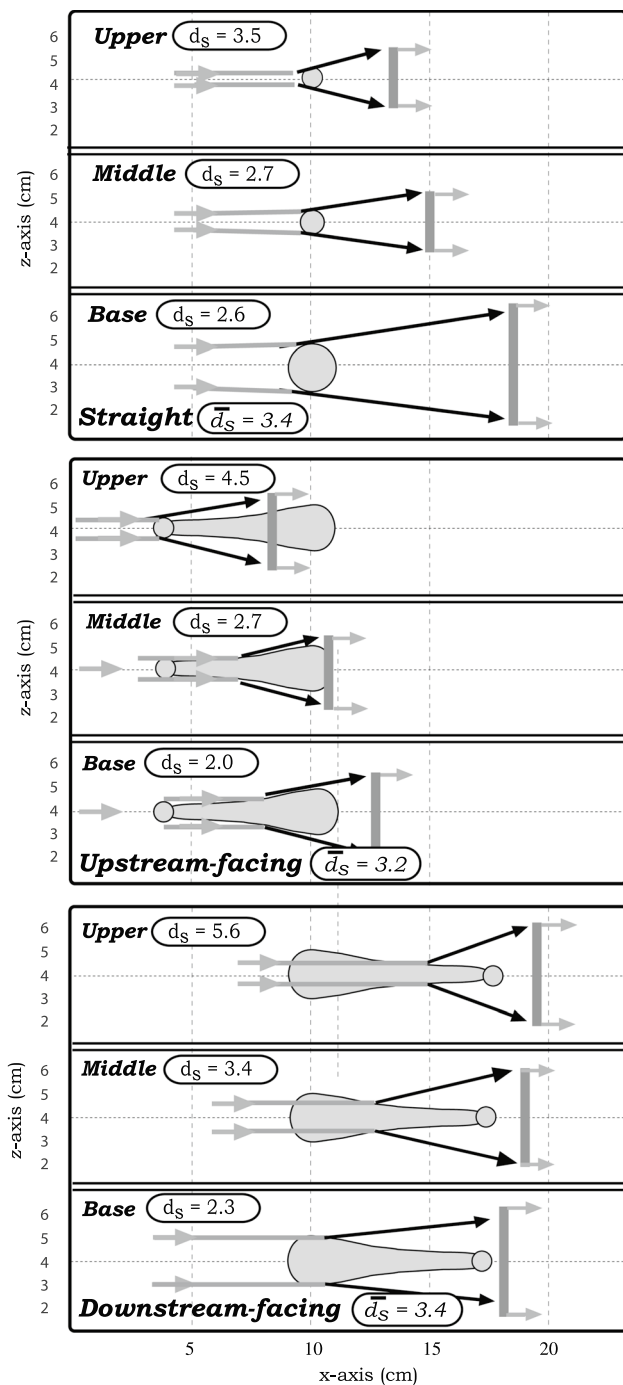


Fig. 8 Horizontal post-encounter spread d_s (dimensionless), of particles encountering the three tentacle postures in the three vertical zones (upper, middle, and base). The spread is indicated by the arrows and bar, after which particles rejoined the freestream, or remained below the model bases ($n=10$ for each zone). Mean d_s shown for each zone and overall mean for each tentacle posture. Note that the origins of the three tentacle postures now share a similar origin for ease of interpretation of the post-encounter spread

zone gave similar retention values in both the *inner* and *outer* horizontal regions (r -value = 1.5).

Upstream-facing tentacle: Average *upper-zone* encounters r -value was 1.6 (Fig. 10) with most particles traveling downward where they were strongly retained in the *inner middle* and *base horizontal regions* (*middle* $r=7.9$, and *base* $r=4.6$). *Middle-zone* encounter particles experienced more uniform retention (*inner* $r=1.2$ and *outer* $r=1.1$), with a consistent higher value in the *outer base region* (r -value = 2.6). *Base-zone* encounters were moderate (*inner* $r=1.2$ and *outer* $r=1.9$); however, particles that dropped below the xz -axis were not recorded.

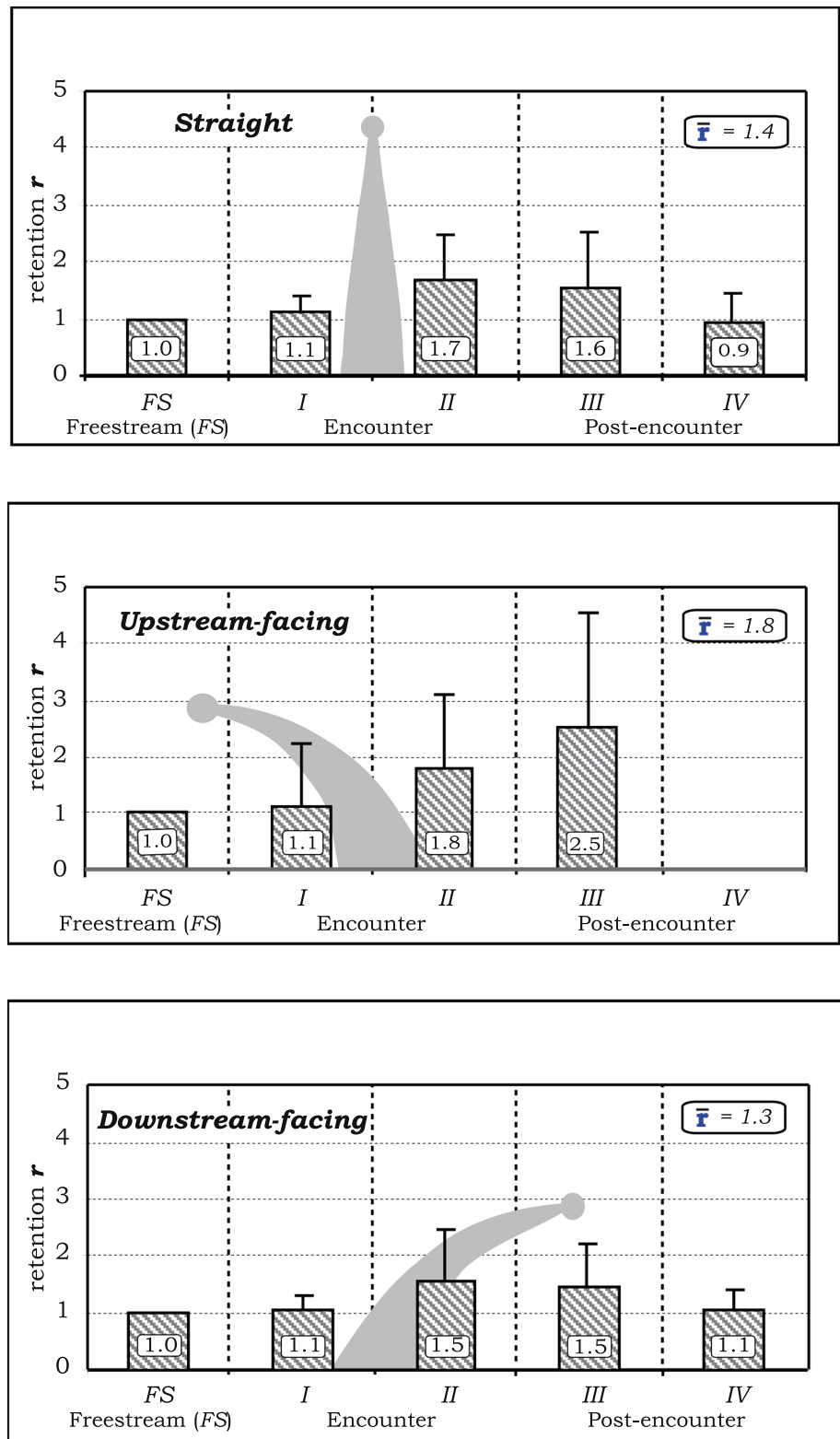
Downstream-facing tentacle. Particles encountering the *downstream-facing* tentacle within the different vertical zones produced very different retention values, but generally produced strong retention, particularly in the *inner vertical zones* for particles approaching the *middle* and *base vertical zones* (Fig. 10). *Upper-zone* particles were only slightly retained close to the lee surface (*inner* $r=1.7$; and *outer* $r=1.8$), and none dropped into lower vertical zones. *Middle-zone* encounters indicated a marked retention and upward influence. Particles spent little time (*inner* $r=1.1$; and *outer* $r=2.7$) in the *middle vertical zone*, but many traveled upwards into the *upper vertical zone* where they experienced strong retention (*inner* $r=10.9$; and *outer* $r=2.5$). Particles approaching the *base vertical zone* demonstrated a similar influence of strong vertically entrainment and retention (*inner* $r=1.8$; and *outer* $r=4.8$). Those that traveled upwards close to the tentacle and were particularly strongly retained in the *middle vertical zone* (*inner* $r=16.8$; and *outer* $r=9.7$), and somewhat less, but still strong in the *upper vertical zone* (*inner* $r=9.2$; and *outer* $r=1.8$). *Outer* retention in the *base* and *middle horizontal regions* was moderate.

Tumbles and contacts

Almost all particles had paths that rotated or looped following an encounter with the tentacle models (Fig. 11a). The vertical *straight* model produced the least events (77%) and the *upstream-* and *downstream-facing* slightly more (87 and 93%, respectively). There was no significant influence of the encounter heights.

For particles that encountered the three tentacle models, 61% contacted the model. Of these, 91% directly impacting the frontal surface and 9% contacted the lee side as they traveled in vortices. Again, there was no significant influence of the encounter heights.

Fig. 9 Retention r -values and standard deviations of particles passing through the horizontal encounter regions of the three tentacle models. (The limitations of the video setup did not permit measurements in the upstream-facing Region IV.) Note that the origins of the three tentacle postures now share a similar origin for ease of interpretation of the post-encounter spread



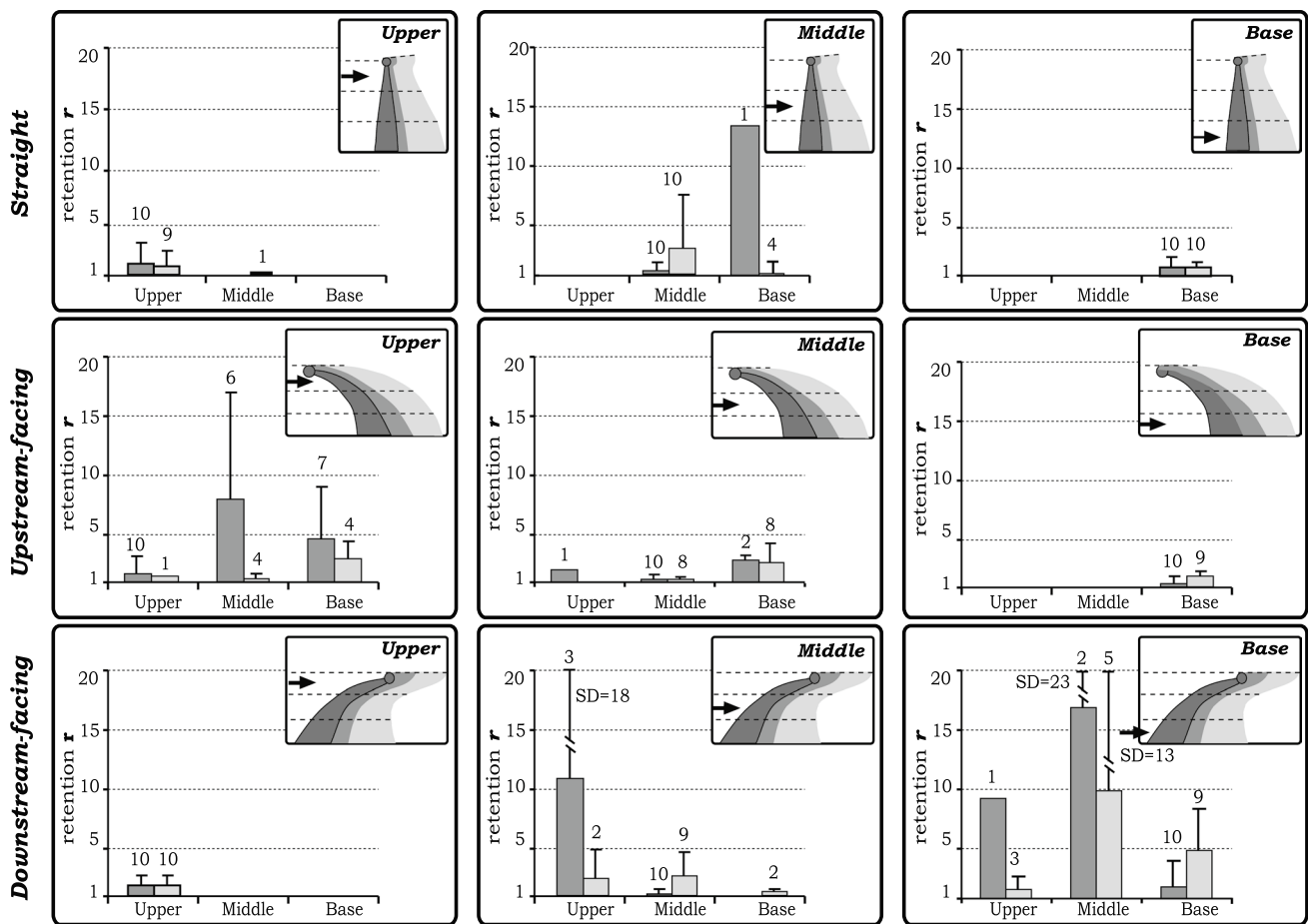


Fig. 10 Retention *r*-values in the inner and outer horizontal regions following particle encounters ($n = 10$) with the different tentacle postures in the three vertical zones (upper, middle, base). N above the

bars indicates the number of particles (of the 10) that were deflected into each horizontal region

Frontal contacts accounted for 100% ($n = 16$) in the *straight* tentacle, 88% ($n = 11$) in the *upstream-facing* tentacle, and 92% ($n = 26$) in the *downstream-facing* tentacle. Overall, the *downstream-facing* tentacle experienced that highest frequency of contact (Fig. 12).

Sweeper tentacle

Almost all the particles (21) that encountered the sweeper tentacle ($n = 24$) tended to travel along the length of the tentacle and remain within the arbitrary “closeness” envelope despite the effects of gravitational fall (Fig. 12a-c). The mean distance away from the tentacle surface was only slightly greater than the local diameter (mean = 1.1; SD = 0.73). Summing the straight-line distances between exit and entry points along the horizontal regions (A–G) indicated that particles followed courses 20% longer than a freestream straight-line path (Fig. 12d). Retention values along the horizontal regions ranged from $r = 1.05$ – 1.43 , with a mean $r = 1.31$ (Fig. 12).

During this travel, particles behaved much differently than if they had remained in the freestream (Fig. 12d). Every particle tumbled, contacted, and crossed over (or under) the tentacle axis at least once. Activity was highest at mid-length, with activity dropping off in the last two regions (Fig. 12f).

Discussion

Flow regimes and length of coral tentacles

A compilation (Table 1) of depth distribution (Goreau and Wells 1967) and ecozones (Liddell and Ohlhorst 1987) did not give a significant correlation between tentacle length and depth ($R^2 = -0.08$). This result suggests that either there is no correlation, or that the data are inadequate to answer the question. However, distribution is apparently further complicated by the role of phenotypic plasticity in some species. Individual colony morphology appears to allow, at least in

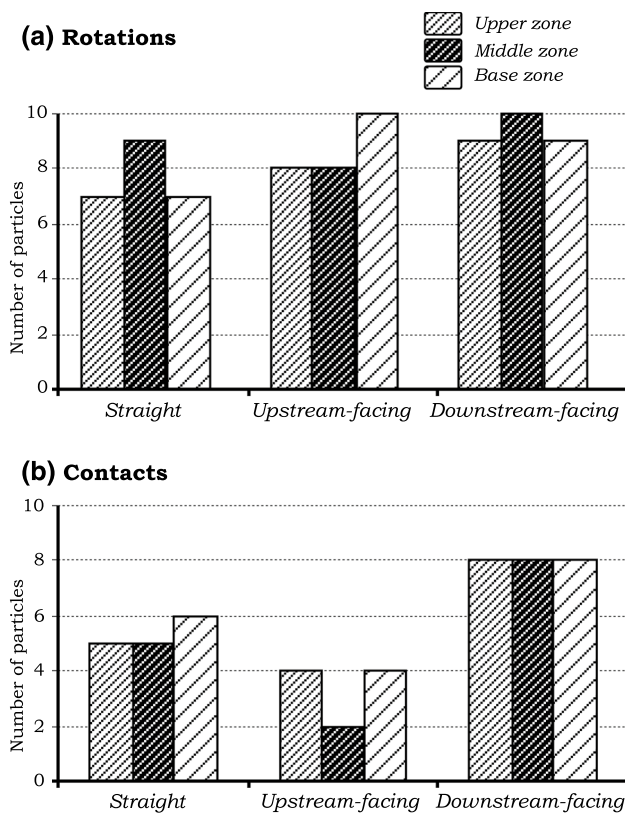


Fig. 11 Rotations (a) and contacts (b) of particles following encounter with tentacle models in each vertical zone

two common Caribbean species, *Madracis mirabilis* (Sebens 1997) and *Agaricia agaricites* (Helmuth and Sebens 1993), to live across a wide depth range of the same Jamaican reefs. *Madracis mirabilis* (2–22 m depth) changes branching in response to the local micro-flow conditions. These studies indirectly support the hypothesis that tentacle length and microscale flow values are linked, but further confirmation will require morphological descriptions of individual colonies, as well as micro-flow measurements at the polyp level.

In the corals examined, tentacle lengths spanned a range of 0.05–1.3 cm, with *sweeper* tentacles up to 4 (*A. agaricites*) and 20 (*M. cavernosa*) times longer (Table 1). The inherent flexibility of tentacles, especially in the mid-range and longer tentacles (0.53–1.2 cm), allows them to bend in response to flow or when feeding (Fig. 13), but in general their postures can be described as either *straight*, or *curved*.

Smaller tentacled corals (0.05–0.23 cm) found in shallow fast-flow environments (10–25 cm s⁻¹) have $Re \sim 100$ –500. The longer (0.36–1.01 cm) tentacled species have Re (300–3000) (Table 1). These values indicate that corals live in a world of turbulent rather than laminar flow (LaBarbera 1984). Although the tentacle models used in this study are in the upper range ($Re = 3500$), they are well within the prerequisite “same order of magnitude” of Re to reflect the same

flow patterns (Vogel 1983). We can assume, therefore, that the microscale flow patterns produced by the models are like those produced by mid-sized coral tentacles.

Particle behavior following encounters with tentacles

Vertical deflection

Near-bed boundary layers in temperate waters have been reported to have strong vertical gradients (Vogel 1983; Nowell and Jumars 1984), and within this narrow layer seston rapidly changes particle concentration and composition, with the lighter, nutrient rich particles found mostly 5 cm above the seabed (Muschenheim 1987). Assuming a similar near-bed boundary layer exists over coral reefs, a vertical extension strategy of feeding elements would appear to be advantageous to many coral species. Indeed, Sebens et al. (1998) found that zooplankton capture in the field was greatly affected by morphology and polyp size and that predation on zooplankton was encounter limited.

The specific postures of tentacles result in significant changes in the vertical deflection over the surface of a coral polyp. The downward deflection of *straight* tentacles increases effective filtering height. In the simple polyps, the strong downward deflection of the *upstream-facing* tentacles would greatly increase particle flux toward the polyp oral region. The strong upward lift from *downstream-facing* posture, on the other hand, may be important in not only keeping particles within the filtering array of tentacles in the contiguous polyps, but prevent particles from accumulating below and between the polyps.

Horizontal encounter width and spread

The encounter width of particles was found to be slightly less than the width of the tentacle. However, given the repetitive nature of the tentacle arrays over the surface of a colony, particles traveling through this array would seem to have a high probability of impacting a tentacle surface. This possibility would become greater as the vertical-*straight* tentacles tend to drive particles downwards where the frontal area of impact increases with the width of the tentacle base. On the other hand, the average post-encounter spread ratio following encounter with a tentacle is large ($d_s = 3.2$), which would cause particles to diffuse across a colony and consequently increase probability of impacting upon a tentacle.

Retention of particles

The finding that particles are retained in the wake of the model tentacles is predicted from basic fluid mechanics, although a “tapered cylinder” is not a simple condition and has not been investigated at these Re s. The vortices formed

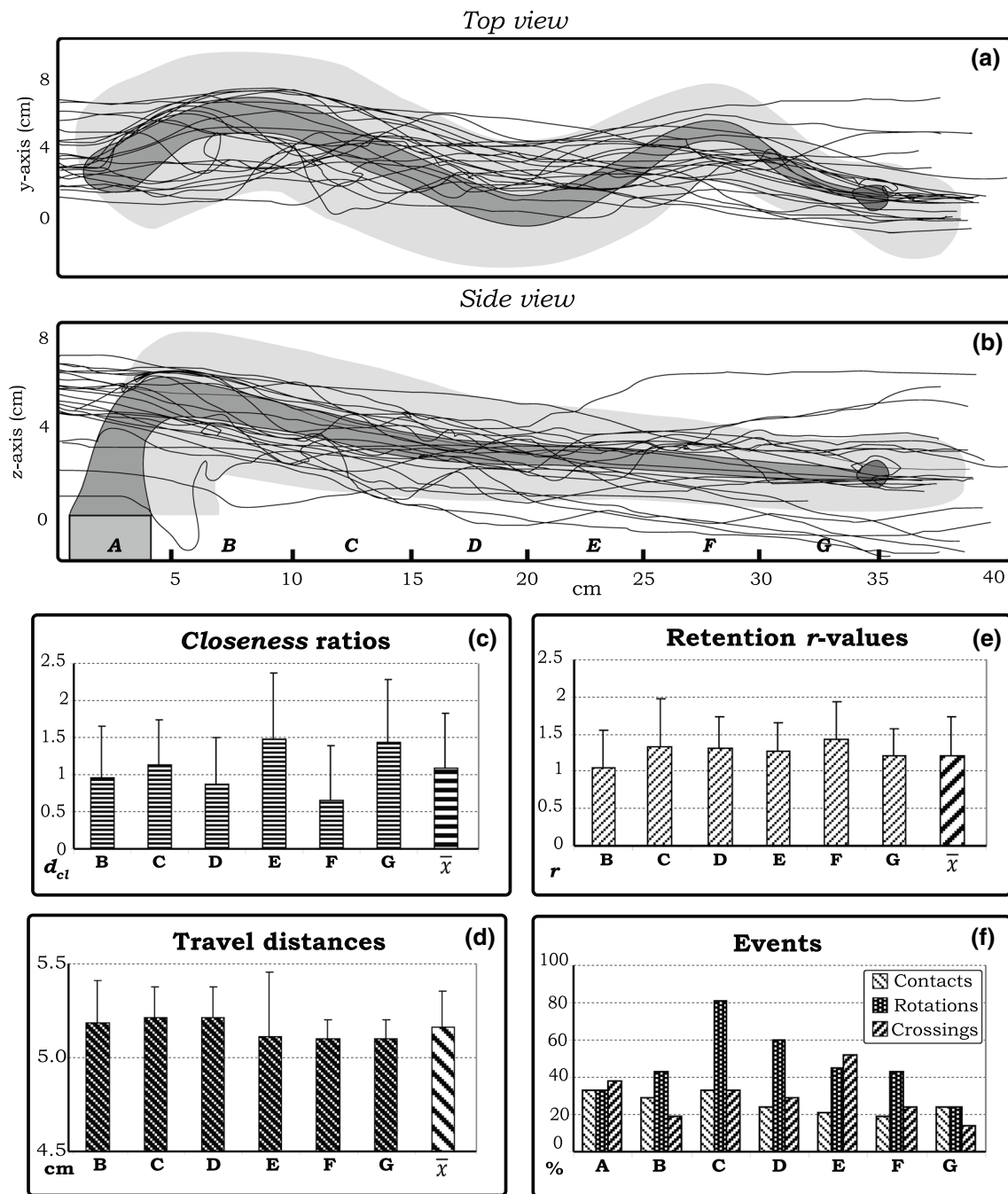


Fig. 12 Tracer particles ($n=24$) around the 35-cm-long sweeper tentacle model. The shaded “closeness” area is 2.0 local diameters wide (a and b). Other sub-figures: c closeness values along tentacle;

d straight-line travel distances between horizontal regions (A-G); e retention r -values; f percentage of particles that contacted, rotated, or crossed the tentacle axis within each horizontal region

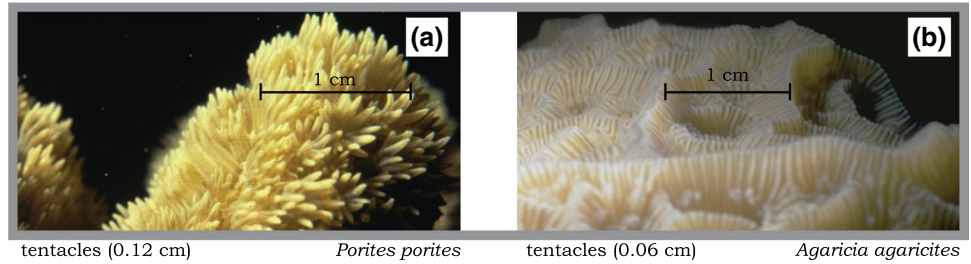
at the lee surface of a cylinder are the agents responsible for the increased “holding time,” and in flow rates over $Re = 40$, they begin to shed irregularly (Vogel 1983; Blevins 1984). Analogous engineering studies have shown that this turbulence increases the heat transfer coefficient within the boundary layer of a cylinder by approximately 80 percent by the continual renewal of “fresh” fluid to the surface by the

turbulent eddies (Kestin et al. 1961). This same mechanism has been hypothesized to be applicable to particle encounter through interception and impaction (Patterson 1991). The empirical results of this study, and in particular the retention values, support this prediction.

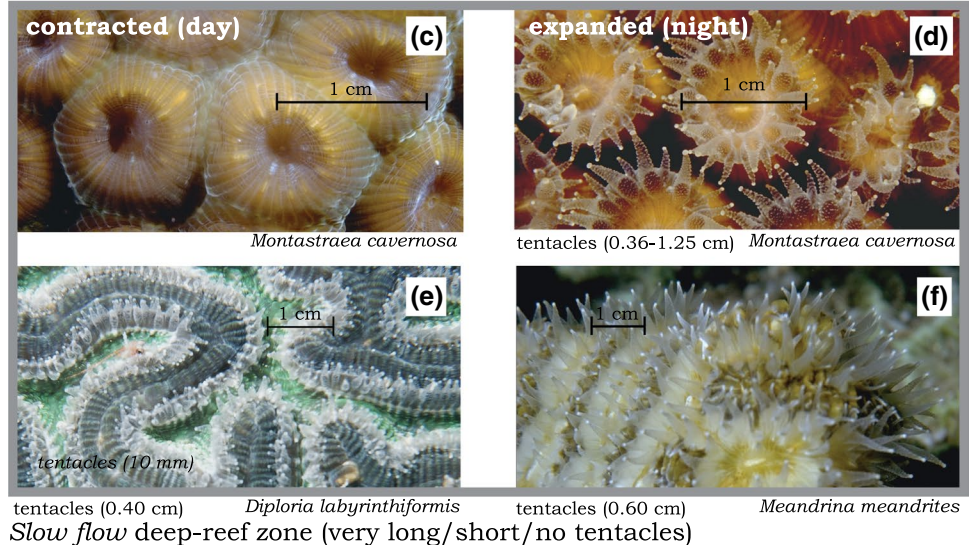
Retention in the immediate post-encounter regions was found for all three tentacle positions. It was particularly

Fig. 13 Examples of common coral species found across a typical Caribbean reef in the shallow-reef (a, b), mid-reef (c, d, e, f), and deep-reef (g, h, i, j) zones, showing the wide variation in soft tissue structure and tentacle sizes

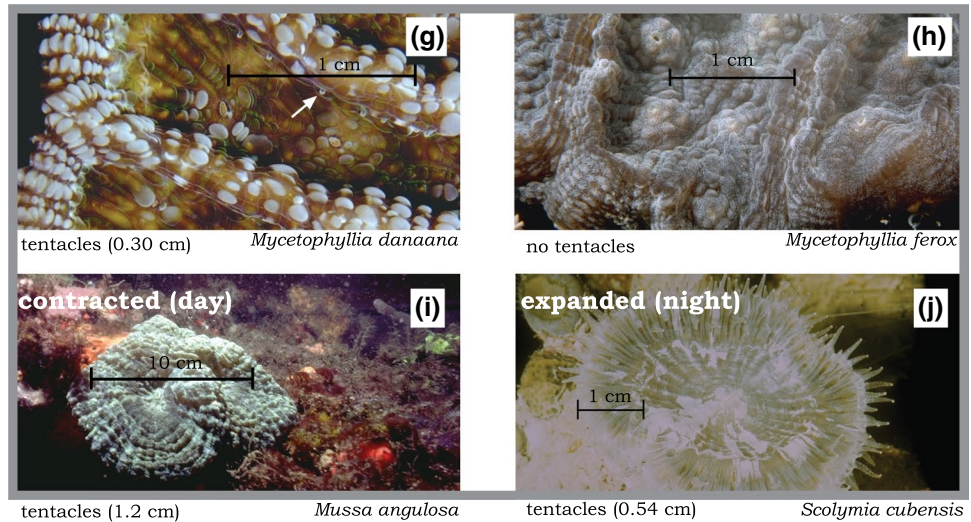
Fast flow shallow reef zone (short tentacles)



Moderate flow mid-reef zone (long tentacles)



Slow flow deep-reef zone (very long/short/no tentacles)



strong in region III behind the *upstream-facing* tentacle ($r=2.5$), compared to the *straight* and *downstream-facing* models where the wake appeared to be disintegrating and retention values dropped to $r=1.6$ and 1.5 , respectively (Fig. 9). Retention of particles 1.5–2.5 times their freestream value has important implications to particle settlement over

oral surfaces. Several species are believed to use mucus as a method of entrapping particles over their oral surface (Lewis and Price 1975) and increase in time would allow for significant settlement of many particles within the seston.

However, closer analysis found that retention was focused within one local tentacle diameter, especially in

the *downstream-facing* tentacle, where retention r -values reached 10.9 in the upward third and 16.8 in the middle regions. This has significant implications to potential feeding success of a suspension feeder, as direct frontal interception of particles on the upstream collecting surface is not necessarily the only opportunity to trap a particle. These leeward vortices hold or often return the particles very close to the tentacle surface.

Rotation and tumbling of particles

All three tentacle postures increased the rotation of particles encountering tentacles. Since direct interception by a feeding element is dependent on particle diameter (Rubenstein and Koehl 1977), rotating and tumbling by any object in the flow field would increase the effective “width” of a particle by extending the particle beyond its freestream path and will increase probability of contact. The turbulence of the vortices results in inherent high standard deviations in all the parameters measured. Larger sample sizes would undoubtedly have reduced them, but despite these constraints, the overall patterns were consistent and have given insight and appreciation of the dynamics.

Capture rates

The results of this study could be incorporated into predictive models of capture rates by polyps, provided that retention efficiencies for particular particle types are assumed (or measured). Shimeta and Jumars (1991) note that maximization of encounter rate *vs.* encounter efficiency is affected differently by flow advection *vs.* size of the particle collector. As they note, “Retention converts encounter into capture and is therefore equally important to study.” Our work provides quantitative insights into the magnitude of localized encounter rate that could thus be used to provide a framework for a predictive capture rate model.

Sweeper tentacles

Sweeper tentacles have been found in several coral species (Price 1973; Chornesky and Williams 1983; Logan 1986; Lang 1973). Although the presence of *sweeper* tentacles is generally described as an aggressive response to contiguous neighbors, the *sweeper* tentacles of the *M. cavernosa* colony photographed in this study was not contiguous with another colony, and some of the polyps with *sweeper* tentacles were central in the colony. It is proposed that these tentacles had been extended for feeding, as results of this study support feeding as a potentially effective strategy.

Particles passing along *sweeper* tentacles remained closer to the tentacle surface, following erratic, but longer paths (20% longer on average), resulting in an overall average

retention r -value = 1.3 (Fig. 12e). In addition, all particles were not only tumbled, but also made contact at least once with the tentacle surface.

The rigid model is most likely to have different results than a live tentacle. Field observations, for example, found that the flexibility of these tentacles allows them to be swept back and forth in the oscillating currents, causing them not only to flutter, pass through a much greater volume of water, and in so doing, probably increase encounter probability.

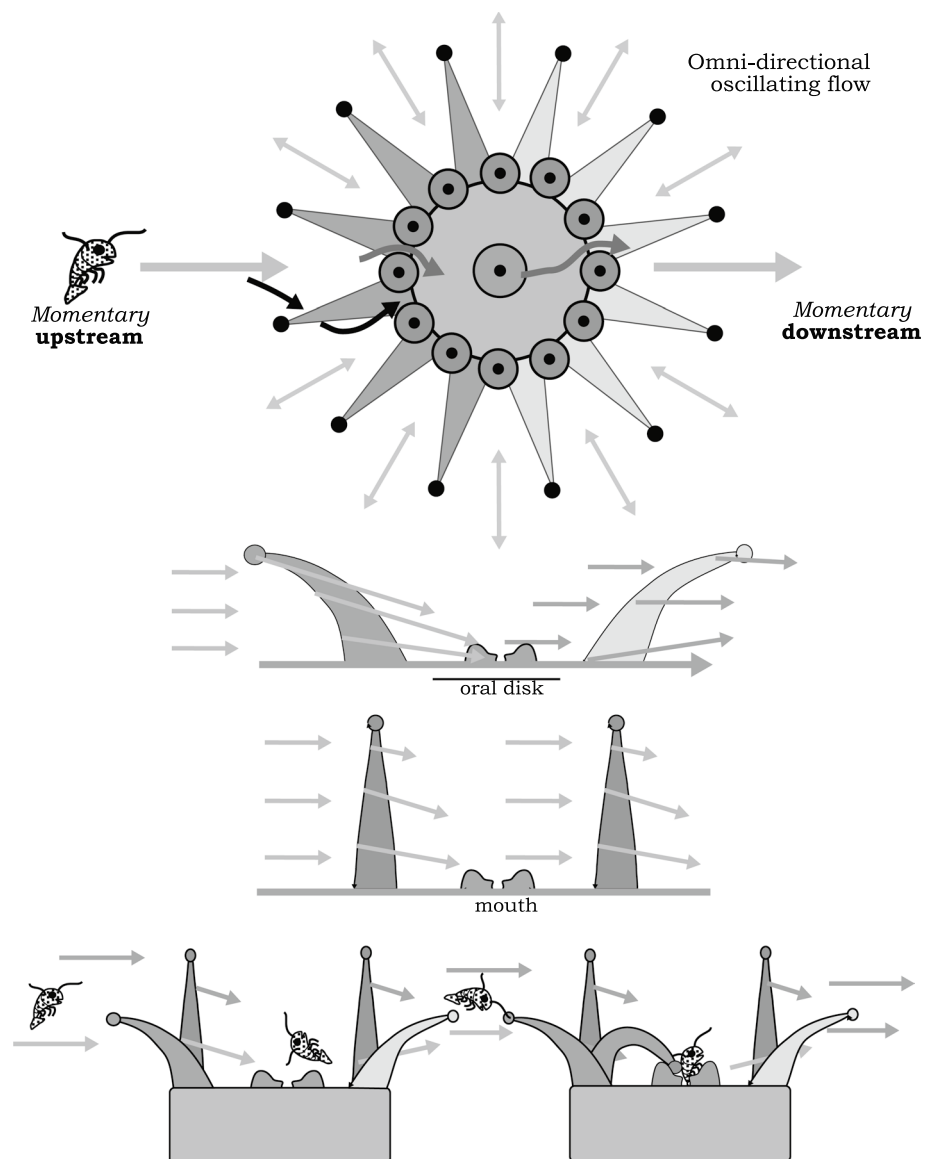
Tentacle combinations in simple and Meandrine Polyps

Coral planulae have bilateral symmetry and research summarized by McFadden et al. (2021) makes a strong case for most Cnidaria as truly bilaterian. We note that after metamorphosis from a planula into a polyp, a secondary radial symmetry appears, and is flow direction independent, probably an adaptation for a sessile lifestyle (Malakhov 2016). In a *simple* polyp, such as *Montastraea cavernosa*, the tentacle whorls around the oral disk are a combination of *straight* and *curved* tentacles (Fig. 14). This configuration would cause particles approaching the upstream side of the polyp to be deflected downward by both the vertical-*straight* and *upstream-facing* tentacles. As the flow continues across the oral disk, the *downstream-facing* and vertical-*straight* tentacles will deflect particles almost horizontally to the next polyp rather than downward between the polyps (Figs. 14, 15). In addition, colonies of simple polyp species generally have curved surfaces; thus, exiting currents would primarily deflect particles directly into the *upstream-facing* and vertical-*straight* tentacles of the adjacent polyp, where again the particles are subjected to further retention and increased probability of contacts and rotation (Fig. 15).

In meandroid corals, tentacle ridges can be described, at least in general, as having a double hedgerow of tentacles on the edge of the thecal walls; one set of vertical-*straight* alternating with a second set of tentacles *curved* inwards across the thecal ridge (Fig. 15). In the composite vector drawing of this scenario, it is proposed that over meandroid polyp surfaces, vertical-*straight* tentacles again would influence particles downward into the thecal valleys where the oral surface and mouths are located. The *curved* tentacles, on the other hand, would seem to keep the thecal wall free from accumulating particles as they deflect particles upward across the thecal wall where they then meet an *upstream-facing* tentacle hedgerow that deflects particles downwards toward the oral valley (Fig. 15). The process is simply reversed with the same results in the next flow oscillation.

To further understand feeding mechanisms and distribution of corals, more information is needed on the microscale flow conditions in the field over individual colonies. Only a few such studies have been made with limited numbers of species, depth ranges, and flow habitats (Shashar et al. 1996;

Fig. 14 Synergistic effect of tentacles and positions found around the oral disk of a simple coral polyp. The "upstream-facing" curved tentacles on the perimeter of the disk are first to encounter the current, along with whatever food packets it is carrying, and they deflect the current downward to the oral disk. As the current exits the oral disk area, it encounters mirror image "downstream-facing" curved tentacles whose base zone deflects current upwards. The current runs directly into the "upstream-facing" tentacles of the adjacent polyp and is re-filtered



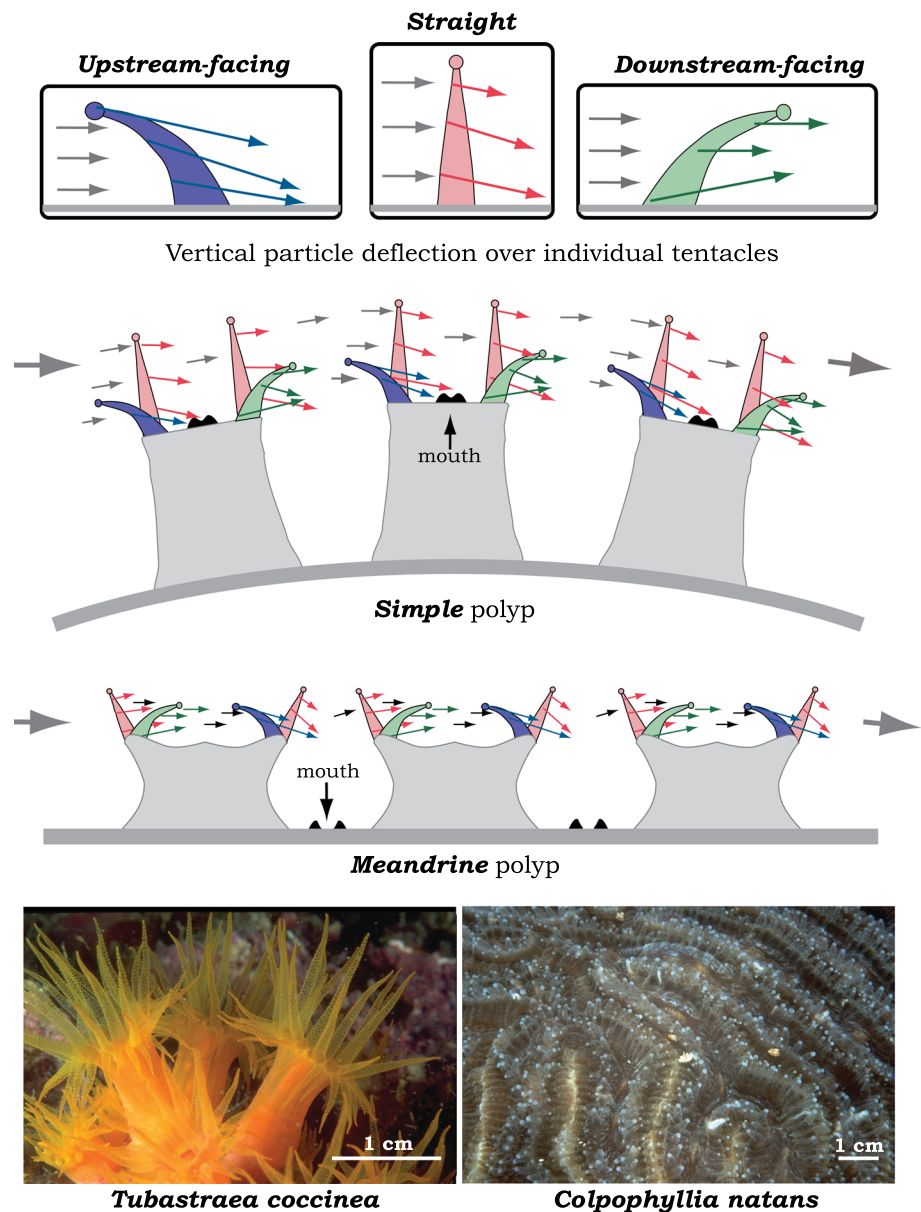
Hench and Rosman 2013; Stocking et al. 2018). Recently, Shavit et al. (2022) achieved in situ measurements using particle image velocimetry (PIV) around a massive species (*Dipsastraea favus*), when the polyps were expanded and contracted. They noted that when tentacles were expanded, the flow altered substantially into a canopy flow (sensu Nepf 2012) very different from the boundary layer flow present when tentacles were contracted. Many of their observations on increased residence time, velocity fluctuations, and mixing around the tentacles are congruent with observations of flow around our flexible models.

A recent review on the turbulence characteristics over coral reefs makes a strong case that such further work is needed, e.g., the role of spatial variation from upstream colony wakes on momentum flux (Gardella and Edmunds 2001; Davis et al. 2021). Hench and Rosman (2013) observed

strong recirculation zones induced by the colonies themselves and enhanced Reynolds stresses in the shear layers around the periphery of wakes. How these colony-induced aspects of the flow field affect particle capture and mass transfer remains an active area of research.

The momentum boundary layer and diffusive boundary layers around corals are affected similarly by details of flow around corals, including the polyps. The momentum boundary layer is about an order of magnitude thicker than the diffusive boundary (Shashar et al. 1996), but both respond to changes in the flow field in a qualitatively similar way. Mass transfer of dissolved substances to coral colonies has been shown to be dependent on morphology and flow regime (Patterson et al. 1991; Patterson 1992a, b). Inasmuch as mass transfer and particle flux respond similarly to the flow field,

Fig. 15 Synergistic composite of vertical particle deflection due to different postures of model tentacles on simple (e.g., *Tubastraea*) and meandrine (e.g., *Colpophyllia*) polyps. Particles deflect toward the oral disks in both models, and oscillating currents simply reverse the flow with the same results



more work is needed on small-scale details of the flow at the level of the polyp. Indeed, laboratory experiments (Reidenbach et al. 2006) and modeling based on field measurements shows the importance of flow in enhancing mass flux in branched coral colonies (Kaandorp et al. 1996; Chang et al. 2014).

Because coral tentacles exhibit such a diversity of shape and size, they most likely have several functions which vary between species. Malul et al. (2020) recently showed that the elasticity of the tentacles results in motions that are out-of-phase with oscillatory flows, thereby enhancing mass transfer around the polyp. Microscale flow modulation by tentacles within polyps is but one of their

functions, and physical modeling allows insight into this process. Future research should integrate studies of coral form and function for both particle capture and mass transfer to better understand the physiological limits to coral performance in this era of climate change.

Acknowledgements We thank the University of California, Davis, Northeastern University, Fulbright Canada, the National Science and Engineering Research Council of Canada, the National Oceanic and Atmospheric Administration's National Undersea Research Program, the Professional Association of Diving Instructors, and S.A. MacTaggart for financial support. We thank A. Theyer for assistance with video analysis, J. Curry for data entry, S. Williams and B. Helmut for discussions, two anonymous peer reviewers and the Topic Editor for helpful suggestions that greatly improved the paper, and J. Chim, Applied Elastomerics Inc., for help with model fabrication.

Funding Open access funding provided by Northeastern University Library.

Declarations

Conflict of interest On behalf of all authors, the corresponding author states that there is no conflict of interest.

Open Access This article is licensed under a Creative Commons Attribution 4.0 International License, which permits use, sharing, adaptation, distribution and reproduction in any medium or format, as long as you give appropriate credit to the original author(s) and the source, provide a link to the Creative Commons licence, and indicate if changes were made. The images or other third party material in this article are included in the article's Creative Commons licence, unless indicated otherwise in a credit line to the material. If material is not included in the article's Creative Commons licence and your intended use is not permitted by statutory regulation or exceeds the permitted use, you will need to obtain permission directly from the copyright holder. To view a copy of this licence, visit <http://creativecommons.org/licenses/by/4.0/>.

References

- Abelson A, Miloh T, Loya Y (1993) Flow patterns influenced by substrata and body morphologies of benthic organisms, and their roles in determining availability of food particles. *Limnol Oceanogr* 38:1116–1124. <https://doi.org/10.4319/lo.1993.38.6.1116>
- Allredge AL, Gotschalk C (1988) In situ settling behavior of marine snow. *Limnol Oceanogr* 33:339–351. <https://doi.org/10.4319/lo.1988.33.3.0339>
- Blevins RD (1984) Applied fluid dynamics handbook. Van Nostrand Reinhold Company Inc, New York
- Butman CA (1986) Larval settlement of soft-sediment invertebrates: some predictions based on an analysis of near-bottom velocity profiles. *Elsevier Oceanogr Ser* 42:487–513. [https://doi.org/10.1016/S0422-9894\(08\)71061-4](https://doi.org/10.1016/S0422-9894(08)71061-4)
- Chang S, Iacocarino G, Ham F, Elkins C, Monismith S (2014) Local shear and mass transfer on individual coral colonies: computations in unidirectional and wave-driven flows. *J Geophys Res Oceans* 119:2599–2619. <https://doi.org/10.1002/2013JC009751>
- Chornesky EA, Williams SL (1983) Distribution of sweeper tentacles on *Montastraea cavernosa*. *Symp Ser Underwater Res* 1:61–67
- Darwin C (1842). The structure and distribution of coral reefs. Smith, Elder & Co., London
- Davis KA, Pawlak G, Monismith SG (2021) Turbulence and coral reefs. *Ann Rev Mar Sci* 13:343–373. <https://doi.org/10.1146/annurev-marine-042120-071823>
- Denny MW (1988) Biology and mechanics of the wave-swept environment. Princeton University Press, Princeton.
- Gardella DJ, Edmunds PJ (2001) The effect of flow and morphology on boundary layers in the scleractinians *Dichoceonia stokesii* (Milne-Edwards and Haime) and *Stephanocoenia michilini* (Milne-Edwards and Haime). *J Exp Mar Biol Ecol* 256:279–289. [https://doi.org/10.1016/s0022-0981\(00\)00326-9](https://doi.org/10.1016/s0022-0981(00)00326-9)
- Gibbs RJ (1985) Estuarine flocs: their size, settling velocity and density. *J Geophys Res C Oceans* 90:3249–3251. <https://doi.org/10.1029/JC090iC02p03249>
- Goreau T, Wells JW (1967) The shallow-water Scleractinia of Jamaica: revised list of species and their vertical distribution range. *Bull Mar Sci* 17:442–453
- Helmuth B, Sebens K (1993) The influence of colony morphology and orientation to flow on particle capture by scleractinian coral *Agaricia agaricites* (Linnaeus). *J Exp Mar Biol Ecol* 165:251–278. [https://doi.org/10.1016/0022-0981\(93\)90109-2](https://doi.org/10.1016/0022-0981(93)90109-2)
- Hench JL, Rosman JH (2013) Observations of spatial flow patterns at the coral colony scale on a shallow reef flat. *J Geophys Res Oceans* 118:1142–1156. <https://doi.org/10.1002/jgrc.20105>
- Jackson GA (1989) Simulation of bacterial attraction and adhesion to falling particles in an aquatic environment. *Limnol Oceanogr* 34:514–530. <https://doi.org/10.4319/lo.1989.34.3.0514>
- Johannes RE (1967) Ecology of organic aggregates in the vicinity of a coral reef. *Limnol Oceanogr* 12:189–195. <https://doi.org/10.4319/lo.1967.12.2.0189>
- Johnson AS, Sebens KP (1993) Consequences of a flattened morphology: effects of flow on feeding rates of the scleractinian coral *Meandrina meandrites*. *Mar Ecol Prog Ser* 99:99–114
- Jokiel PL (1978) Effects of water motion on reef corals. *J Exp Mar Biol Ecol* 35:87–97. [https://doi.org/10.1016/0022-0981\(78\)90092-8](https://doi.org/10.1016/0022-0981(78)90092-8)
- Kestin J, Maeder PF, Sogin HH (1961) The influence of turbulence on the transfer of heat to cylinders near the stagnation point. *J Appl Math Phys* 12:115–132. <https://doi.org/10.1007/BF01601012>
- LaBarbera M (1984) Feeding currents and particle capture mechanisms in suspension feeding animals. *Am Zool* 24:71–84. <https://doi.org/10.1093/icb/24.1.71>
- Lang JC (1973) Interspecific aggression by scleractinian corals. 2. Why the race is not only to the swift. *Bull Mar Sci* 23:260–279
- Lewis JB, Price WS (1975) Feeding mechanisms and feeding strategies of Atlantic reef corals. *J Zool Lond* 176:527–544. <https://doi.org/10.1111/j.1469-7998.1975.tb03219.x>
- Liddell WD, Ohlhorst SL (1987) Patterns of reef community structure, north Jamaica. *Bull Mar Sci* 40:311–329
- Logan A (1986) Aggressive behavior in reef corals: a strategy for survival? *Sea Frontiers* 32:347–351
- Malakhov VV (2016) Symmetry and the tentacular apparatus in Cnidaria. *Russ Jour Mari Biol* 42:287–298. <https://doi.org/10.1134/S1063074016040064>
- Malul D, Holzman R, Shavit U (2020) Coral tentacle elasticity promotes an *out-of-phase* motion that improves mass transfer. *Proc R Soc B* 287:20200180. <https://doi.org/10.1098/rspb.2020.0180>
- McFadden CS, Quattrini AM, Brugler MR, Cowman PF, Dueñas LF, Kitahara MV, Paz-García DA, Reimer JD, Rodríguez E (2021) Phylogenomics, origin, and diversification of Anthozoans (Phylum Cnidaria). *Syst Biol* 70:635–647. <https://doi.org/10.1093/sysbio/syaa103>
- Muscatine L, Hand C (1958) Direct evidence for the transfer of materials from symbiotic algae to the tissues of a coelenterate. *Proc Natl Acad Sci USA* 44:1259–1263. <https://doi.org/10.1073/pnas.44.12.12>
- Muscatine L, Porter JW (1977) Reef corals: mutualistic symbiosis adapted to nutrient-poor environments. *BioSci* 27:454–459. <https://doi.org/10.2307/1297526>
- Muschenheim DK (1987) The dynamics of near-bed seston flux and suspension-feeding benthos. *J Mar Res* 45:473–496. <https://doi.org/10.1357/00224087788401098>
- Nepf HM (2012) Flow and transport in regions with aquatic vegetation. *Ann Rev Fluid Mech* 44:123–142. <https://doi.org/10.1146/annurev-fluid-120710-101048>
- Nowell ARM, Jumars PA (1984) Flow environments of aquatic benthos. *Ann Rev Ecol Syst* 15:303–328. <https://doi.org/10.1146/annurev.es.15.110184.001511>
- Patterson MR (1984) Patterns of whole colony prey capture in the octocoral, *Alcyonium siderium*. *Biol Bull* 167:613–629. <https://doi.org/10.2307/1541414>

- Patterson MR (1991) The effects of flow on polyp-level prey capture in an octocoral, *Alcyonium siderium*. *Biol Bull* 180:93–102. <https://doi.org/10.2307/1542432>
- Patterson MR (1992a) A mass transfer explanation of metabolic scaling relations in some aquatic invertebrates and algae. *Science* 255:1421–1423. <https://doi.org/10.1126/science.255.5050.1421>
- Patterson MR (1992b) A chemical engineering view of cnidarian symbioses. *Am Zool* 32:566–582. <https://doi.org/10.1093/icb/32.4.566>
- Patterson MR, Sebens KP, Olson RR (1991) *In situ* measurements of flow effects on primary production and dark respiration in reef corals. *Limnol Oceanogr* 36:936–948. <https://doi.org/10.4319/lo.1991.36.5.0936>
- Porter J (1974) Zooplankton feeding by the Caribbean reef coral *Montastrea cavernosa*. *Proc. 2nd Int. Symp Coral Reefs* 1:111–125
- Price WS (1973) Aspects of feeding behaviour of West Indian reef corals. MSc Thesis, McGill University
- Reidenbach MA, Koseff JR, Monismith SG, Steinback JV (2006) The effects of waves and morphology on mass transfer within branches reef corals. *Limnol Oceanogr* 51:1134–1141. <https://doi.org/10.4319/lo.2006.51.2.1134>
- Rubenstein DI, Koehl MAR (1977) The mechanisms of filter feeding: some theoretical considerations. *Am Nat* 111:981–994
- Salzen EA (1957) The density of sea urchin eggs, embryos and larvae. *Exp Cell Res* 12:615–625. [https://doi.org/10.1016/0014-4827\(57\)90177-5](https://doi.org/10.1016/0014-4827(57)90177-5)
- Sebens KP (1984) Water flow and coral colony size: interhabitat comparisons of octocoral *Alcyonium siderium*. *Proc Natl Acad Sci USA* 81:5473–5477. <https://doi.org/10.1073/pnas.81.17.5473>
- Sebens KP, Done TJ (1992) Water flow, growth form and distribution of scleractinian corals: Davies Reef (GBR) Australia. In: *Proceedings of 7th International Coral Reef Symposium*, vol 1, pp 557–568
- Sebens KP, Johnson AS (1991) Effects of water movement on prey capture and distribution of reef corals. *Hydrobiologia* 226:91–101. <https://doi.org/10.1007/BF00006810>
- Sebens KP, Witting J, Helmuth B (1997) Effects of water flow and branch spacing on particle capture by the reef coral *Madracis mirabilis* (Duchassaing and Michelotti). *J Exp Mar Biol Ecol* 211:1–28. [https://doi.org/10.1016/S0022-0981\(96\)02636-6](https://doi.org/10.1016/S0022-0981(96)02636-6)
- Sebens KP, Grace SP, Helmuth B, Maney EJ Jr, Miles JS (1998) Water flow and prey capture by three scleractinian corals, *Madracis mirabilis*, *Montastrea cavernosa* and *Porites porites*, in a field enclosure. *Mar Biol* 131:347–360. <https://doi.org/10.1007/s002270050328>
- Shashar N, Kinane S, Jokiel PL, Patterson MR (1996) Hydromechanical boundary layers over a coral reef. *J Exp Mar Biol Ecol* 199:17–28. [https://doi.org/10.1016/0022-0981\(95\)00156-5](https://doi.org/10.1016/0022-0981(95)00156-5)
- Shavit S, Mass T, Genin A (2022) The small-scale flow field around *Dipastraea favus* corals. *Front Mar Sci* 9:857109. <https://doi.org/10.3389/fmars.2022.857109>
- Shimeta J, Jumars PA (1991) Physical mechanisms and rates of particle capture by suspension-feeders. *Oceanogr Mar Biol Ann Rev* 29:191–257
- Stocking JB, Laforsch C, Sigl R, Reidenbach MA (2018) The role of turbulent hydrodynamics and surface morphology on heat and mass transfer in corals. *J Roy Soc Interface* 15:20180448. <https://doi.org/10.1098/rsif.2018.0448>
- Vogel S (1983) *Life in moving fluids: the physical biology of flow*. Princeton University Press, Princeton. <https://doi.org/10.1515/9780691212975>

Publisher's Note Springer Nature remains neutral with regard to jurisdictional claims in published maps and institutional affiliations.